Journal of Molecular Catalysis A: Chemical 315 (2010) 108–134

Contents lists available at ScienceDirect

Journal of Molecular Catalysis A: Chemical

journal homepage: www.elsevier.com/locate/molcata

Temporal analysis of products (TAP)—Recent advances in technology for kinetic analysis of multi-component catalysts

John T. Gleaves[a], Gregory Yablonsky[a,b,*], Xiaolin Zheng[a], Rebecca Fushimi[a], Patrick L. Mills[c]

[a] Department of Energy, Environmental, and Chemical Engineering, Washington University in St. Louis, 1 Brookings Drive, St. Louis, MO 63130, USA
[b] Parks College of Engineering, Department of Chemistry, Saint Louis University, 3450 Lindell Blvd, St. Louis, MO 63103, USA
[c] Department of Chemical and Natural Gas Engineering, Frank H. Dotterweich College of Engineering, Texas A&M University-Kingsville, 700 University Blvd, MSC 188, Kingsville, TX 78363-8202, USA

ARTICLE INFO

Article history:
Available online 26 June 2009

Keywords:
Temporal analysis of products (TAP)
Heterogeneous catalysis
Kinetics
Transient methods
Gas–solid reactions
Knudsen diffusion
Time-of-flight mass spectrometer
Atomic beam deposition
Single particle experiments
Pressure gap

ABSTRACT

This paper presents an overview of the evolution, advancements, and capabilities of the temporal analysis of products (TAP) reactor system as a unique catalyst characterization tool. The origination of the TAP reactor based on molecular beam scattering experiments is briefly mentioned. The advancement in TAP reactor design from the TAP-1 system to the TAP-3 system is introduced to highlight its relevance as a valuable tool for elucidating mechanistic and kinetic aspects of adsorption, diffusion, and reaction in gas–solid systems. Since the invention of the TAP reactor system, a series of TAP microreactor configurations has been introduced with different amounts of catalyst packing starting from the one-zone microreactor to the most recent introduction, the single particle microreactor in which a single Pt particle is packed among 100,000 inert quartz particles. An advantage to decreasing the catalyst zone inside the microreactor is to eliminate non-uniformity in the active zone while still achieving high conversions (95%). Experimental designs and results coupling the TAP reactor to other experimental systems such as a time-of-flight mass spectrometer and atomic beam deposition system is also presented. Key results from recent TAP experiments are presented to show how the TAP reactor is used to answer fundamental questions in catalysis such as bridging the pressure gap between industrial catalysis and surface science, understanding the surface lifetimes of reactive adspecies in TAP pump-probe experiments, finding kinetic rate constants related to changes in catalyst composition and its performance.

1. Introduction

Over the next several decades, a new generation of catalytic materials and processes will be needed to meet the increasing demands for fuel, food, chemicals, pharmaceuticals, and a whole host of materials (e.g., plastics and fibers). New catalysts will also play a pivotal role in environmental remediation and halting global warming. Currently, the petroleum-based process industry generates products that have an annual worldwide production value exceeding 4 trillion dollars. Heterogeneous catalysis and multiphase reaction engineering are the technology engines that power the chemical and fuel industries since nearly 75% of all chemicals, polymers, and advanced materials are produced with the aid of catalysts. In addition, over 90% of newly developed processes involve catalysis, and over 95% of industrial reactors are based on heterogeneous catalytic processes. How to supply the vast quantities of fuels, and chemicals when oil is no longer readily available is one of the most challenging and important problems now facing humanity. An essential piece of the puzzle is the development of new approaches to unravel the tangle of processes that occur on complex industrial catalysts.

Despite advances in surface science and computational chemistry that provide molecular level insight into surface physics and chemistry, catalyst development for realistic processes still relies extensively on empirical methods and trial and error processes. Generally the method used to develop practical catalysts follows the catalyst development cycle (CDC) illustrated in Fig. 1. In the first step of the CDC, candidate materials are selected to test as catalysts. In step two, the materials are synthesized, and in steps three and four, the materials are tested for catalytic activity, and characterized structurally.

The CDC includes a decision branch, which is reached through steps three and four. This branch gives rise to a number of cyclic paths. The path depicted by the red arrows represents a key cycle in the CDC, and provides crucial performance information used to determine if the cycle can be exited. In practice, however, information gained in a single cycle of the CDC often does not provide guidance for the next step. In many cases, a cycle only provides

* Corresponding author at: Department of Energy, Environmental, and Chemical Engineering, Washington University in St. Louis, 1 Brookings Drive, St. Louis, MO 63130, USA.
E-mail address: gregoryyablonsky@yahoo.com (G. Yablonsky).

1381-1169/$ – see front matter © 2009 Elsevier B.V. All rights reserved.
doi:10.1016/j.molcata.2009.06.017

Nomenclature

a_s	surface concentration of active sites (mol/cm^2 of catalyst)
A	cross-sectional area of the microreactor (cm^2)
α	ratio of total number of active centers and number of molecules of gas A in the pulse
C_A	concentration of gas A (mol/cm^3)
$\overline{C}_A$	dimensionless concentration of gas A
D_e	effective Knudsen diffusivity (cm^2/s)
D_{eA}	effective Knudsen diffusivity of gas A (cm^2/s)
δ_z	delta function with respect to axial coordinate z
δ_ζ	delta function with respect to dimensionless axial coordinate ζ
ε_b	fractional voidage of the packed bed inside microreactor
F_A	flow of gas A at microreactor outlet (mol/s)
$\overline{F}_A$	dimensionless flow of gas A at microreactor outlet
H_p	peak height of the normalized gas exit flow
k_a	adsorption rate constant (cm^3/mol s)
k'_a	adsorption rate constant (s^{-1})
$\overline{k}_a$	dimensionless adsorption rate constant
k_{ads}	apparent adsorption constant (s^{-1})
k_d	desorption rate constant (s^{-1})
$\overline{k}_d$	dimensionless desorption rate constant
k_a	dimensionless modified kinetic constant of adsorption
L	length of the microreactor (cm)
L_{II}	length of diffusion zone II (cm)
ΔL	thickness of the catalytic zone (cm)
M	molecular mass
N_{pA}	number of moles or molecules of gas A in the input pulse
R	universal gas constant
S_v	surface area of catalyst per volume of catalyst (cm^{-1})
t	time (s)
t_p	time at which the gas exit flow is at a maximum (s)
τ	dimensionless time
τ_p	dimensionless time at which gas exit flow is at a maximum
τ_{res}^{conv}	residence time for convective flow in CSTR (s)
$\tau_{res,cat}^{dif}$	residence time for diffusion through the catalytic zone in thin-zone TAP microreactor (s)
T	temperature (K, °C)
θ_A	fractional surface coverage
$\overline{\theta}_A$	pulse normalized surface concentration
V_{void}	void volume inside microreactor (cm^3 gas/cm^3 catalyst)
X	conversion
z	axial coordinate (cm)
ζ	dimensionless axial coordinate

negative information such as a particular catalyst synthesis leads to an inactive or non-selective candidate. Generally, a large number of iterations, often involving the preparation of perhaps thousands or tens-of-thousands of catalyst samples, precede the finalization of a new catalyst formulation.

Two general strategies have been used in an effort to accelerate the rate of catalyst invention when fundamental guidance or previous data is either absent or has failed to produce a viable catalyst candidate. One strategy is focused on decreasing the CDC cycle time by decreasing the time required to synthesize and evaluate the performance of new catalyst samples. In this case, emphasis is placed on rapid screening of many different catalyst compositions to determine promising candidates that can be further developed. The combinatorial catalyst or so-called high-throughput approach represents the most advanced example of this strategy [1–4].

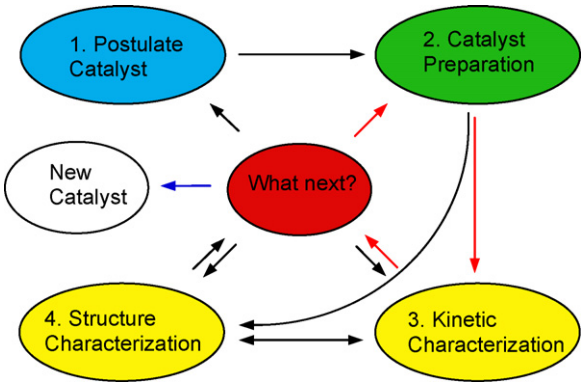

Fig. 1. Catalyst development cycle.

The second strategy is focused on making the CDC more efficient by increasing the quantity and quality of information obtained in each cycle. Information that links changes in kinetic properties to changes in the structure of a catalyst sample is very valuable. An example of the second strategy is the use of surface science techniques to characterize different catalyst samples after reaction to determine if differences in surface composition and catalyst performance can be related.

Understanding how the catalytic activity and selectivity of a substance is related from the composition and structure of the substance is a fundamental problem in the field of catalysis. Solving the problem involves finding relationships between kinetic data and structural data. Relationships that provide a link between the reaction kinetics and the structure of the "active catalytic site" are particularly important because they provide essential information for explaining how catalytic systems work, and for creating new or improved catalysts.

To develop an activity–structure relationship for a gas–solid catalytic system, it is necessary to obtain kinetic data that can be directly related to the structure/composition of the solid catalyst, especially the catalyst's surface. For reactions involving technical catalysts (e.g., supported metals or mixed-metal oxides), acquiring such kinetic data presents a formidable challenge since the reaction kinetics and the catalysts are typically very complex. Moreover, in many cases, and particularly in the case of mixed-metal oxides, the structure/composition of the catalyst is influenced by the reaction mixture and can undergo changes as a function of time-on-stream. This has obvious implications during extended studies involving investigations on kinetics and mechanism.

Kinetic testing of technical catalysts is normally performed at industrial conditions. It is common to prepare a series of catalyst samples with different compositions and/or structures, and then test the samples at the same reaction conditions to determine differences in catalytic activity. The samples are also characterized using one or more structural techniques. To obtain an activity–structure relationship, the differences in activity are matched against the structural information. Sometimes, a well-characterized standard catalyst is used for comparison purposes. The goal of this procedure is to discover a correspondence between the measured activity and some structural characteristic. One obstacle to developing an activity–structure relationship using this methodology is that the measured kinetics generally reflects the global characteristics of the catalytic process rather than the local characteristics of the active catalytic sites. Also, during reaction, a catalyst can change so that the observed kinetics is not represen-

tative of one specific catalyst state. Such changes can occur during kinetic testing, and it is difficult to distinguish different catalyst states with most existing kinetic testing procedures.

According to the methodology of surface science, reactions are carried out over a well-defined surface (e.g., a specific plane of a metal single crystal), so that the observed kinetics can be directly associated with the structure of the surface [5–8]. Surface science techniques are used to define the structure of the crystal surface, and to determine if a surface is changed by reaction. Information pertaining to reaction-induced changes can be obtained by characterizing a surface before and after reaction. Kinetics are obtained by thermal desorption techniques or from scattering experiments. The kinetics often reflects the intrinsic reactivity of the specific crystal plane being studied. By comparing the reactivities of different crystal planes of the same metal, inferences can be drawn regarding the nature of the active catalytic site.

Surface science techniques [5–8] can be used to characterize the structure or composition of technical catalysts; however, direct kinetic testing of technical catalysts in surface science systems is usually impractical. Structural and compositional data from surface science experiments may be matched with data from atmospheric pressure kinetics, but the heterogeneous surface structure of technical materials prevents the observed kinetics from being directly associated with a specific crystal plane or surface structure. Also, the structure of a technical catalyst may change when it is moved from atmospheric pressure conditions (esp. when the catalyst has been exposed to a reactive mixture) to high vacuum conditions. In this case, the structural data may not be directly related to the actual active site.

Experiments commonly used to obtain kinetic data at industrial reaction conditions are usually based on a steady-state approach. An important advantage of this approach is that it can be readily applied to technical catalysts. The steady-state approach has disadvantages, however, when it comes to developing activity–structure relationships. First, steady-state kinetic data is usually related to only the slow steps of a complex kinetic process, and does not provide detailed information. Second, the observed kinetics is a complex function of the gas-phase composition, the structure/composition of the solid, and other process variables. As a result of these factors, details of the gas–solid reaction, and detailed activity–structure relationships, cannot be readily established using steady-state kinetic data.

The surface science approach provides a procedure for relating the surface structure of a solid to the reaction kinetics that occurs on the solid surface. Consequently, surface science studies can provide activity–structure relationships. On the other hand, surface science experiments are performed at ultrahigh vacuum conditions using well-defined model surfaces (e.g., metal single crystals), and are not well suited for investigating kinetics on technical catalysts.

A well-known problem that arises when attempting to compare data from more practical studies with data from surface science studies is the so-called "pressure gap" problem first delineated by Bonzel [9]. He noted that the large difference in pressures (often greater than 9–10 orders-of-magnitude), and the difference between single crystals versus technical catalysts makes it very difficult to compare results from the two experimental regimes. In fact, despite enormous strides in understanding how reactions occur on well-defined surfaces, large gaps exist in our fundamental understanding of how reactions occur on "real" surfaces. Such surfaces exhibit a complex multi-scale structure with critical dimensions ranging from the microscopic to the atomic scale, and are not well suited for study using ultrahigh vacuum surface science techniques.

Many industrial catalyst particles are composed of metals deposited on metal oxides or mixed-metal oxide microcrystallites bound together in a random orientation. A typical catalyst particle will contain a complex pore structure with pore dimensions in the micron size range. In addition to the crystalline phase or phases, catalysts may contain one or more amorphous phases deposited on the surface of the crystalline phases. The surfaces of the crystallites are composed of different crystal planes containing a variety of defects such as kinks, edges, steps, and vacancies. Defects may range in size from microns to Angstroms (Å). The chemical composition of a surface may be different from the underlying crystal bulk, and can change under reaction conditions. In the case of metal oxides, there is a lack of knowledge regarding surface reactions even on well-defined surfaces [10]. In the case of "real" oxides, surface reactions at defect sites may dominate the chemistry, and these types of reactions are particularly difficult to study by surface science techniques.

Under reaction conditions, the kinetic state of a catalyst can change. For example, the absolute number of active sites can change as a result of a change in the catalyst surface area, a change in the crystal morphology, or a change in surface oxidation state. During reaction, the available number of active sites can change as a result of adsorption. The specific reactivity of sites can change because the composition or structure of the sites changes. A process that causes a change in the number of active sites may also cause a change in structure of the active sites. In this case, the changes may even compensate one another. Such effects complicate the problem of determining the number of active sites on a catalyst and their specific reactivity. Consequently, to simplify the problem of determining the number of active sites and the kinetic characteristics of individual sites, the experimental strategy that is used should provide a means of maintaining the catalyst in a constant state or should involve a change that is "insignificant".

Since Bennett and Kobayashi–Kobayashi times, it is well accepted in the heterogeneous catalysis literature that transient experiments can provide more mechanistic information about the reaction intermediates and pathways of the various elementary steps when compared to steady-state experiments [11–13,155,164–167]. Steady-state kinetic experiments can reveal the performance of a catalyst after it has evolved into a stable structure. Non-steady-state kinetic experiments reflect changes in performance that occur during the evolution process from one state to another state. The changes in kinetic properties can be related to changes in catalyst composition and structure. However, non-steady-state experiments utilizing continuously stirred tank reactors have been plagued by a number of obstacles, e.g., macroscale hydrodynamic non-uniformity in catalyst bed. In the Bennett review (1999) [167], it was concluded that "it is no longer advantageous to do these experiments in an ideal mixed-flow reactor". See a detailed analysis of this problem in [148].

A new approach for characterizing the catalytic activity of technical and model catalysts called "interrogative kinetics" (IK) [14] combines vacuum pulse-response experiments, commonly known as TAP experiments [14–16], with atmospheric pressure steady-state and transient experiments, and allows a single catalyst sample [17,18] to be tested over a wide domain of pressures (10^5–10^{-6} Pa) and relaxation times (10^3–10^{-4} s) [14,16]. The specific transport domain in which kinetic data are obtained in TAP experiments (Knudsen diffusion domain) is located on the boundary of the surface science domain. The approach is applicable to both model and realistic catalysts, and provides a procedure for bridging the pressure gap [9].

The IK approach uses two types of experiments, called "state-defining" (SD) and "state-altering" (SA) experiments to probe different states of a catalyst sample. In a SD experiment, the catalyst composition and structure change insignificantly during a kinetic test. In a SA experiment, the catalyst composition is changed in a controlled manner. The IK approach involves kinetic testing of a catalyst, and systematically altering its composition or structure in a well-defined process. For example, the oxygen composition of

some metal oxides can be altered in a precisely measurable fashion by heating the oxide in an oxygen atmosphere. After the catalyst composition is incrementally changed, its kinetic characteristics are measured and matched with the composition or structural change. The kinetic measurement is performed under non-steady-state conditions in such a way so as to not significantly alter the kinetic properties of the sample, and to give intrinsic kinetic information. The observed kinetics can be directly correlated with the observed composition change. The approach provides an experimental and theoretical methodology for determining the number of active sites on technical metal oxide catalysts, and a method for measuring the intrinsic kinetic characteristics of the active sites. The IK approach uses a combination of TAP vacuum pulse response and steady-state and transient experiments carried out at atmospheric pressures.

The primary objective of this paper is to review the experimental and theoretical basis of the TAP reactor system along with recent and emerging aspects of the technology. Emphasis is placed upon the physical basis for the TAP experiment and its relationship with molecular beam experiments, the state-of-the-art for TAP reactor systems and recent advances in a next-generation system, developments in coupling a TAP reactor with a time-of-flight mass spectrometer and other analytical systems, mathematical models that can be used for interpretation of the transient responses for extraction of adsorption and kinetic rate parameters, and selected recent applications. A recent special issue of Catalysis Today [15] was dedicated to the TAP reactor with an emphasis upon applications of the technology over the past 10–15 years to various catalytic systems to which the reader is referred.

2. The TAP experiment

2.1. Overview

The Temporal Analysis of Products, or TAP experiment was conceived in the late 1970s to study catalytic reaction mechanisms on industrial catalysts [14,16,19,20]. The initial thought was to devise a simplified "molecular beam" experiment for multi-component catalysts (e.g., mixed-metal oxides and supported metals) that have high surface areas and complex pore structures. Molecular beam scattering (MBS) experiments [21–31] can provide fundamental information on surface structure, reaction dynamics, the elementary steps of a reaction, and the kinetic parameters of individual steps. When used in conjunction with surface characterization techniques, data from a MBS experiment can establish the link between kinetic properties and surface structure. On the other hand, MBS experiments use planar or decorated planar targets to take advantage of the spatial characteristics of the beam. Industrial catalysts have complex surfaces, are composed of multi-component mixtures of different metal oxides or metals combined with metal oxides, and are generally not suitable for MBS experiments. The goal of early TAP designs was to retain the time-dependent features of a molecular beam experiment, minimize gas-phase interactions, and provide a way to extract intrinsic kinetic information from reactions on bulk catalysts. The TAP experiment can be viewed as a bridge between MBS experiments and conventional microreactor experiments.

A variety of MBS setups have been described in the literature, and they generally fall into two different classes: (1) systems designed to study gas-surface dynamics, and (2) systems designed to study the kinetics and mechanism of surface reactions [6].

Fig. 2(a) presents a simplified diagram showing key components of a MBS apparatus. In a typical experiment a well-collimated beam of molecules having a known translational energy is directed toward a target surface, and the velocity and angle distributions

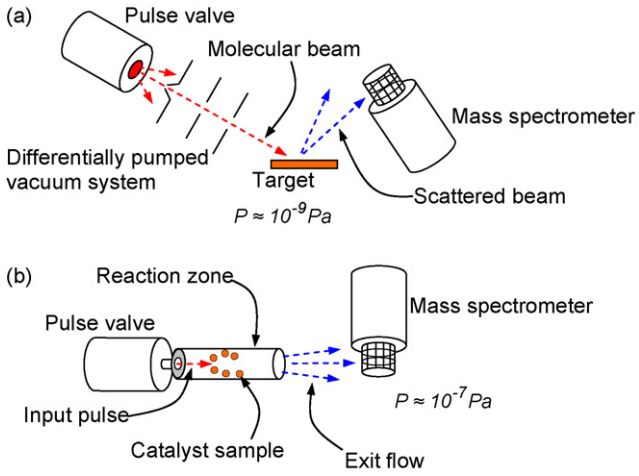

Fig. 2. Conceptional comparison of key components of (a) molecular beam scattering experiment and (b) TAP experiment.

of the scattered molecules are measured. Molecular beam experiments are performed under single collision conditions so that reactant molecules collide once with the target surface but not with each other. The observed distributions contain dynamic information, which describes the process of energy exchange between gas and surface atoms, as well as kinetic and mechanistic information. Scattered molecules from a collimated beam may also exhibit diffraction effects, which provide information on surface structure and bond lengths [21–31].

2.2. TAP reactor setup

A basic TAP setup, depicted in Fig. 2(b), has some characteristics common to an MBS experiment, and others common to conventional microreactor experiments. The key components are a "reaction zone" or microreactor, a fast-pulse gas feed system, a mass spectrometer detector, and a high-throughput ultrahigh vacuum system. The reaction zone (Fig. 2), which holds the catalyst sample, is a temperature controlled cylindrical tube usually made of stainless steel, inconel, or quartz. One end of the tube receives input from the feed system, and the opposite end is open to vacuum. During an experiment the reaction zone and catalyst sample are continuously evacuated. The reaction zone can hold practical catalysts, which are commonly studied in conventional microreactor experiments, as well as single particles, single crystals, or model catalysts, which are studied in MBS experiments.

MBS experiments obtain essential kinetic and mechanistic information by modulating the reactant flux, and measuring the shift in arrival times at the detector between scattered reactant and product molecules. The difference in arrival times can be used to determine reaction sequences, surface lifetimes of adspecies, and rates of surface reactions. TAP pulse-response experiments [14,16,19,20,32,33] extract kinetic information in a similar manner. Injection of a narrow gas pulse into the reaction zone initiates an experiment. The gas molecules travel through the reaction zone where they encounter the catalyst and can react to form product molecules. Molecules that exit the reaction zone are monitored by the mass spectrometer positioned at the outlet. An experiment ends when the flow of reactant and product molecules is no longer detected by the mass spectrometer. The observed characteristic feature in a TAP experiment is the time-dependent gas flow $F(t)$ [moles/s] or [molecules/s] that escapes from the exit of the microreactor. The flow dependencies also have integral characteristics that are related to the moments of the "flow-time" dependencies [14,16,34]. Kinetic and mechanistic information is

obtained by analyzing these dependencies, and gas transport is used as a "measuring stick" to determine the rates of chemical transformations.

In addition to kinetic and mechanistic information, TAP experiments have been used to study transport processes in porous materials, such as zeolites, and oxygen diffusion in metal and metal oxide catalysts. The temperature dependence of TAP transient response curves provides intrinsic rate parameters that can be associated with the surface composition of a catalyst. The number of active sites can be determined in TAP titration experiments.

2.3. Types of TAP experiments

In both TAP and MBS experiments, the sample is maintained under vacuum conditions, which strongly promote desorption of adspecies. Prior to performing a TAP experiment, it is common to heat the catalyst sample and monitor the desorption spectrum. During the heating process, adspecies (e.g., water, CO, CO_2, etc.), which cover the surface at ambient pressures, vacate the surface leaving the coverage to more closely resemble that of an MBS target. Conversely, pulsing a specific species into the reaction zone can increase its coverage so that it resembles coverage at ambient pressures. Pulsing different molecules in an alternating sequence can adjust the surface coverage of two or more species. As a result, coverage in a TAP experiment can be manipulated to resemble coverage in an MBS experiment or coverage in a conventional microreactor experiment.

The input pulse in a TAP experiment typically contains $\approx 10^{14}$ molecules, and the local pressure in an empty reaction zone may reach $\approx 10^{-1}$ Pa during a pulse. If unimpeded, an oxygen molecule can traverse the reaction zone in under 100 μs. If the reaction zone is filled with particles the pressure may reach ≈1.33 Pa in the void spaces if no adsorption occurs. The mean free path in an empty reaction zone is about half the length of the reactor. In an empty reactor, molecules move in beam-like fashion and suffer relatively few collisions. In a packed reactor, the mean free path is ≈4000 μm, which is significantly larger than the space between particles. As a result, in a packed-bed reactor molecules collide with particles, but seldom with one another (Fig. 3).

At sufficiently small pulse intensities, a one-pulse TAP experiment can be considered a state-defining experiment. The number of molecules in a reactant pulse is typically much smaller (10^2–10^5 times smaller) than the number of surface atoms in the catalyst sample being probed [14]. As a result, the reactant pulse does not significantly perturb the catalyst surface.

2.4. TAP reactor applications

Table 1 provides an overview of TAP reactor applications, and the types of catalytic materials that have been studied including supported metals, mixed-metal oxides, zeolites, metal particles, metals deposited on screens, catalytic monoliths, and nanoparticles or atoms deposited on microparticles, single crystals, and other model catalysts.

3. The TAP reactor system

The temporal analysis of products (TAP) reactor system was first patented by the Monsanto Company in 1986 as a novel device for studying the kinetics and mechanisms of heterogeneous catalyzed gas-phase reactions by using a transient response technique with submillisecond time resolution [19]. Two years later in 1988, open literature publications by Monsanto catalyst scientists described how the TAP reactor system was used to elucidate the mechanisms for several heterogeneous catalytic reactions having commercial significance [16,20]. Particular reactions that were studied included *n*-butane oxidation to maleic anhydride over vanadium–phosphorus oxide (VPO) catalysts, propylene oxidation to acrolein over bismuth–molybdates, methanol ammoxidation to HCN over $MnPO_x$ and $FeMoO_x$, and ethylene epoxidation over silver metal [95,96]. In 1989, Monsanto granted an exclusive license to manufacture and sell a commercial version of the TAP reactor to Autoclave Engineers of Erie, PA. Later in that same year, DuPont became the first chemical company in the United States to purchase a TAP reactor from Autoclave Engineers for the newly established Corporate Catalysis Center in Central Research and Development [20]. Later, the TAP-1 system was redesigned and simplified and

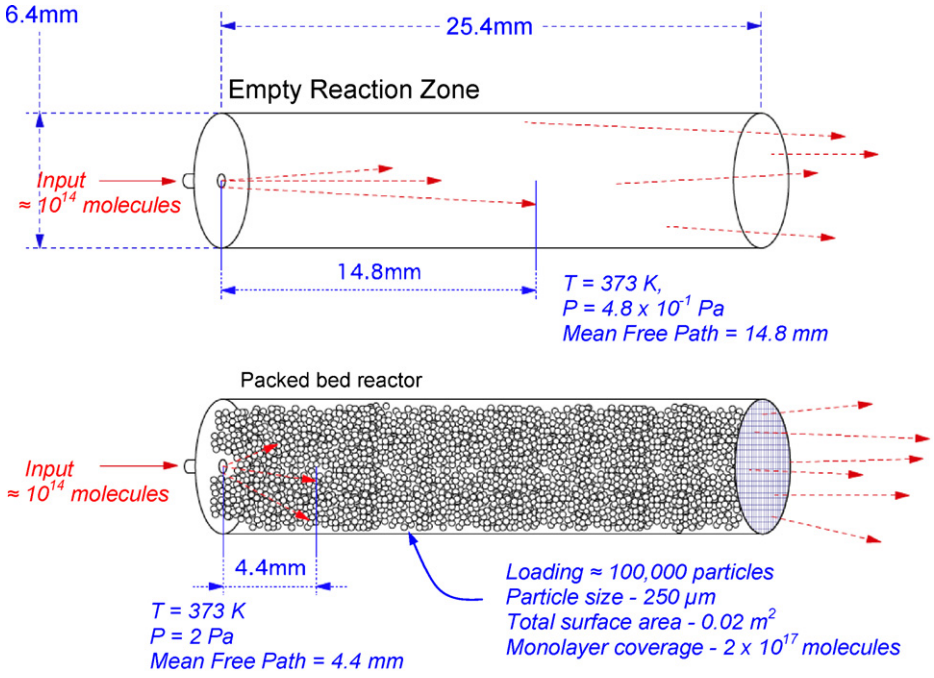

Fig. 3. Scale drawing of a TAP "reaction zone" and packed-bed microreactor containing a loading of nonporous spherical particles ≈250 μm in diameter.

Table 1
Applications and theory of the TAP reactor including the corresponding catalytic materials tested.

Research area	Catalytic materials	References
Reactor transport (adsorption and diffusion)	Zeolites, γ-Al_2O_3, Rh/Al_2O_3, sulfated ZrO_2	[35–42]
Conversion of simple hydrocarbons		
Ethane	Pt/Al_2O_3, Na/CaO, Sm_2O_3/CaO, Sm_2O_3	[43,44]
Methane	MgO, Na/CaO, Sm_2O_3, Ni/Al_2O_3	[45–51]
Conversion to syngas	Rh/γ-Al_2O_3, Pt/MgO, Pt gauzes, Ru/Al_2O_3, Pt/ZrO_2, Pt/Al_2O_3	[52–55]
n-Butane	$VOPO_4$, $(VO)_2P_2O_7$	[56–60]
n-Pentane	$(VO)_2P_2O_7$	[57]
Propane	$VCrMnWO_x$, Fe-ZSM-5, mixed vanadia-based oxides, VO_x/MgO, Sm_2O_3, VO_x/γ-Al_2O_3, Al-Sb-V-W-oxide catalyst	[61–67]
Cracking/reforming of hydrocarbons	Zeolite-based catalysts, Pt-supported catalysts, MgO-Ru/C	[68–73]
Environmental catalysis		
N_2O abatement	Pt, Pt-Rh mixed catalysts, Fe-MFI	[74–78]
NO_x storage	Pt/BaO/Al_2O_3	[79]
SCR of NO_x	Ag/Al_2O_3, Pt/ZSM-5, mordenite	[80–82]
VOC	U_3O_8	[83]
Hydrogenation reactions		
Acrolein hydrogenation	Ag/SiO_2	[84]
Oxidation reactions		
Ammonia oxidation	Pt, Pt–Rh mixed catalysts	[85–89]
CO oxidation	Au/Fe_2O_3, Au/$Ti(OH)_4$, $La_{1-x}Sr_xFe(Pd)O_3$, Pt, Pd/SiO_2	[17,90–94,154,161,169]
Ethylene oxidation	Ag powder	[95,96]
o-Xylene oxidation	VO_x/TiO_2	[97]
Propene oxidation	$Co_{10}Mo_{12}FeBiO_x$, γ-bismuth molybdate	[98–100]
Soot oxidation	La^{3+}-doped CeO_2, CeO_2	[101–103]
Toluene ammoxidation	α-$(NH_4)_2[(VO)_3(P_2O_7)]_2$	[104]
Toluene oxidation	VO_x/TiO_2, VO_x/SiO_2	[105–107]
TAP theory and modeling		[14,16,18,32,34,96,100,108–124,168]

eventually developed into the TAP-2 reactor system [14], which was commercialized by Mithra Technologies. The TAP-3 system retains the basic design of the TAP-2, but is a fully automated instrument that can be operated either locally or remotely via the Internet.

3.1. TAP apparatus design

Fig. 4 presents a simplified schematic of a TAP-3 reactor system, and Fig. 5 shows a photograph of a system. The TAP-3 reactor is comprised of (1) a pulse-valve manifold assembly that supplies gas reactants for pulsed and flow experiments at user defined temperatures and pressures, (2) a microreactor assembly that can be operated isothermally or in a temperature programmed mode, (3) a mass spectrometer detector contained in a high-throughput ultra-high vacuum system, and (4) a computer based control and data acquisition system.

The pulse-valve manifold contains one continuous flow valve and four high-speed pulse valves that are arranged to minimize the dead volume between the valves and the microreactor. The four pulse valves can be triggered simultaneously or in a programmed alternating sequence. Pulse intervals can be varied from microseconds to minutes. Switching between feeds is accomplished electronically and can occur almost instantaneously. The continuous flow valve is connected to a separate manifold containing four flow controllers. The flow controllers and pulse valves can be operated simultaneously.

The TAP-3 vacuum system is comprised of two chambers separated by a pneumatically operated gate-valve, which is closed in the standby position. The lower chamber is evacuated by a 40 cm diameter diffusion pump and associated mechanical pump. The chamber contains a cylindrical liquid nitrogen trap and adjustable baffle that closes when data is not being acquired. The upper chamber holds the mass spectrometer and is pumped by a turbo molecular pump. The background pressure in the mass spectrometer chamber is typically $\approx 10^{-7}$ Pa.

The microreactor is positioned directly above the ionizer of the mass spectrometer, and is attached to a movable stainless steel bellows. A unique rotary-valve assembly is located between the ionizer and the microreactor. It permits the microreactor to be operated at vacuum conditions or atmospheric pressures, and allows the reactor to be removed from the system without venting the vacuum chambers. The reactor can be easily and rapidly switched from one kinetic regime to another without exposing the catalyst sample to the atmosphere.

When the rotary-valve is closed, the TAP microreactor can be operated as a continuous plug flow-type reactor at atmospheric or higher pressures. In the "high-pressure" mode, the bulk of the reactor effluent exits through an external vent. A small amount can be leaked into the vacuum chamber through a variable leak valve. The leaked material can be monitored with the mass spectrometer. In high-pressure experiments, the mass signal usually changes relatively slowly, and can be collected in a scan mode. In this mode, a complete mass spectrum can be acquired about once every 0.25 s. After performing an experiment at atmospheric pressures, the microreactor can be quickly switched to vacuum conditions by opening the rotary-valve.

With the rotary-valve in the open position, all of the reactor effluent vents into the vacuum chamber. The movable bellows allows the reactor outlet to be positioned within 2 mm of the ionizer so that most of the effluent passes through the ionizer. As a result, very small inputs of gas can be detected, with a very high signal to noise (S/N) ratio (Fig. 6). The high S/N ratio allows accurate calculation of the zeroth, first, and second moments of the response curves, and direct determination of many important kinetic characteristics.

For example, reactant conversion for a series of pulses can be determined from the zeroth moment. This change in conversion can be related to a change in the concentration of the active catalytic species. The following quantities can be directly calculated from 0th, 1st, and 2nd moments: Conversion, selectivity, product

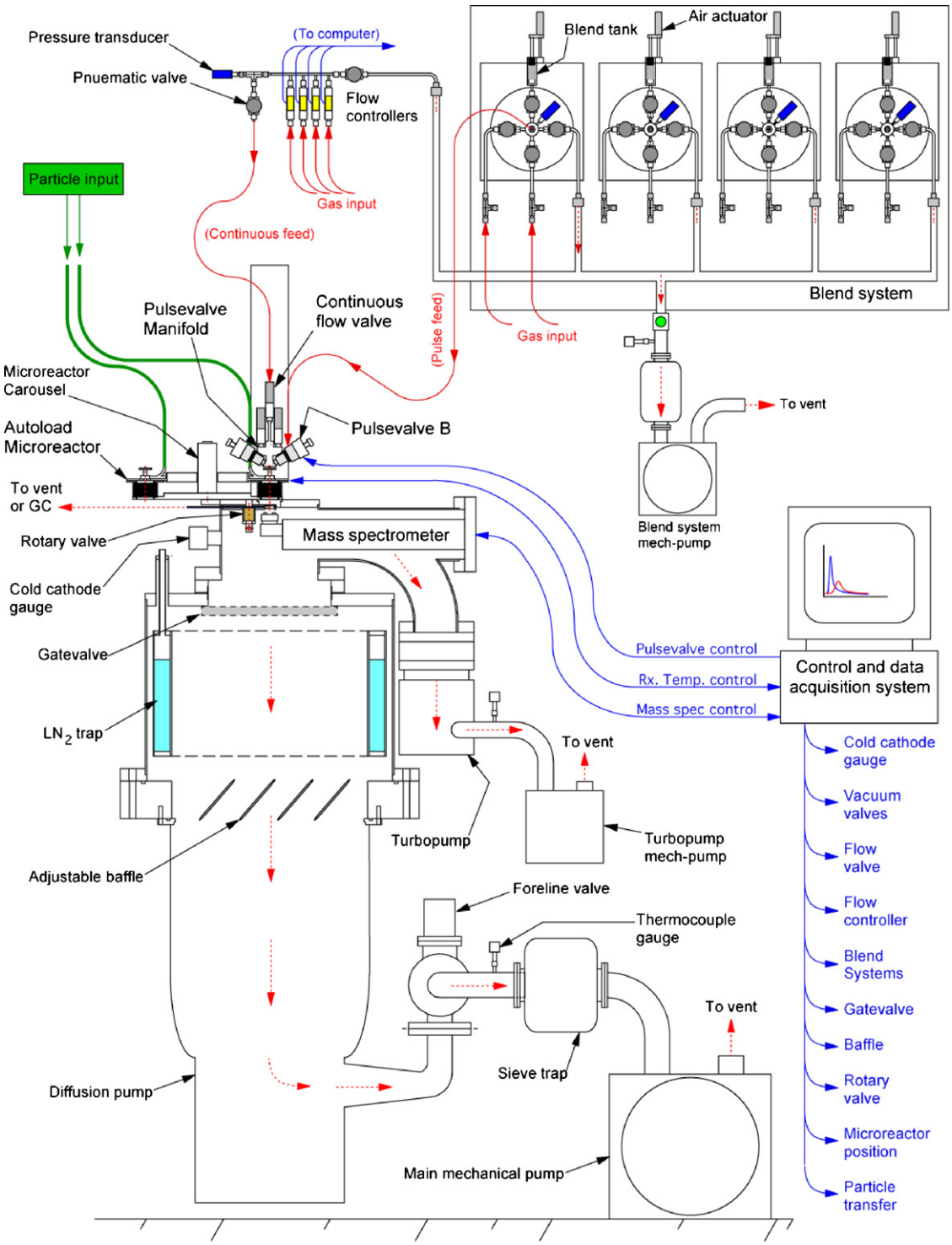

Fig. 4. Schematic of TAP-3 apparatus showing two-chamber vacuum system (base pressure = 10^{-7} Pa) with gate-valve, adjustable baffle, liquid nitrogen trap, rotary-valve for switching between vacuum and pressure experiments, and quadrupole mass spectrometer; microreactor carousel with autoload microreactors and catalyst sample input lines; reactant feed manifold with high speed pulse valves and continuous flow valve; gas feed system with heatable mass flow controllers, heated blend tanks for preparing gas mixtures, and vacuum pump; computer control and data acquisition system indicating main control lines.

yield, residence time, apparent equilibrium and rate constants, and apparent time delay.

The TAP-3 system can accommodate microreactors of different lengths (up to 25 cm) and diameters (up to 2 cm), which are useful for handling a variety of catalyst forms (see Fig. 7). A standard TAP microreactor is constructed of type 316 stainless steel and can be operated at atmospheric pressures or at vacuum conditions. Reactors are heated electrically and the reactor temperature controller provides an array of control options, which include constant temperature operation, programmed heating or cooling at a user defined rate, and the ability to perform multistep ramp-soak programs. The standard microreactor can be heated to 800 °C. Microreactors have also been fabricated from inconel and quartz which allow operation to temperatures as high as 1000 °C.

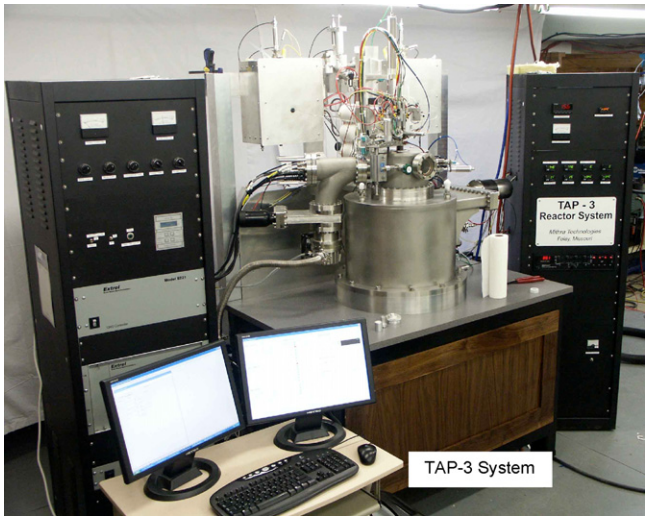

Fig. 5. TAP-3 system.

The TAP-3 menu of experiments includes, but is not limited to, high-speed vacuum pulse-response experiments (TAP Knudsen pulse-response experiments, TAP pump-probe experiments, and TAP multipulse experiments, pulse experiments with a change of time within a pulse and between pulses), atmospheric pressure steady-state, step-transient and SSITKA experiments, temperature programmed desorption (TPD), and temperature programmed reaction (TPR). In addition, newly developed software allows the user to create programmed experimental sequences, which can be stored in memory, and then performed automatically. Sequences may include complex temperature treatments, switching back and forth between atmospheric pressure and vacuum experiments, switching from continuous flow to transient response experiments, or combinations of step-transient, pulse transient, steady-flow, and temperature programmed experiments.

When the TAP-3 system is operated in the high-pressure mode, it can automatically perform a sequence of atmospheric pressure experiments, including temperature programmed (TPD, TPR and TPO) experiments, step response experiments, and steady-state isotopic switching (SSITKA) experiments. Some examples of these are provided in the references cited earlier in Table 1.

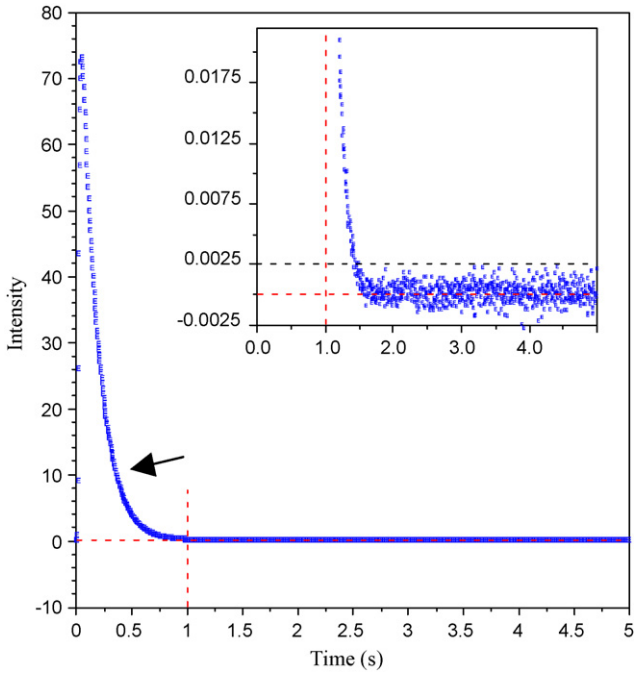

Fig. 6. TAP pulse response curve with inset showing the noise magnitude in the tail of the response. Signal to noise ratio is >30,000 to 1.

4. TAP reactor: advanced analytical systems

4.1. Overview and motivation

The study of reaction mechanisms and kinetics for gas-phase heterogeneous catalyzed systems requires both qualitative identification and quantitative analysis of various gas-phase and surface species as a precursor to development of robust kinetic models. However, most catalytic reactions, especially those that occur in many practical industrial gas-phase catalytic processes, often generate a complex distribution of primary and secondary gas-phase reaction products through a sophisticated sequence of surface-catalyzed reactions whose surface processes and mechanisms are generally not well-understood. For this reason, practicing engineers that must either design new catalytic processes, or

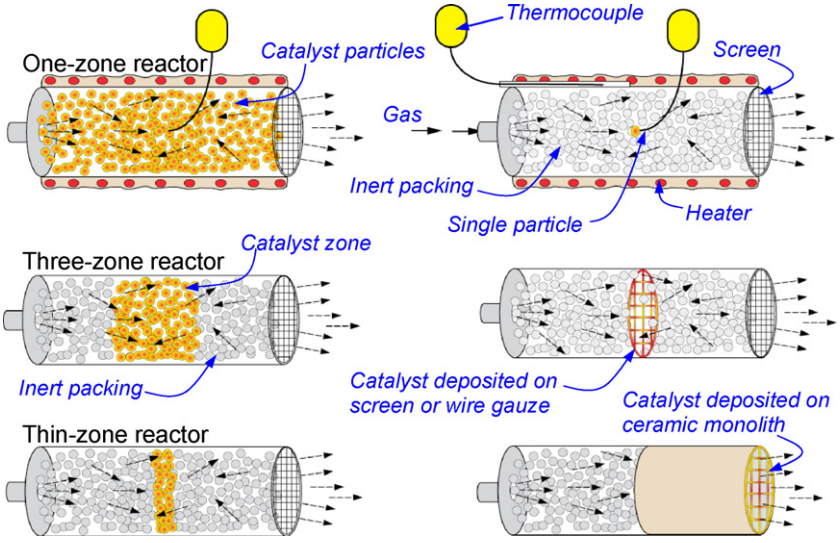

Fig. 7. Examples of TAP packed-bed microreactor configurations and catalyst forms. See Fig. 22 for schematic of TAP system with pulse valves, slide valve, and mass spectrometer.

optimize existing ones, often develop kinetic models based upon empirical power-law, classical Langmuir–Hinshelwood (LH), or Hougen–Watson (HW) rate expressions using kinetic data generated from steady-state flow-type catalytic reactors, such as packed-bed microreactors [125]. Approaches based on mechanisms involve sequences of elementary steps where the precise nature of catalyst active sites is not identified. These rate forms provide a well-known approach for fitting reaction kinetic data, but do not provide a fundamental basis for design of new multi-functional catalyst materials using advanced principles of inorganic, solution-phase and computational chemistry along with supporting advanced surface characterization methods. Experimental reaction studies involving model compounds on well-characterized catalyst surfaces provide one alternate approach for developing insight in reaction mechanisms for these complex systems. However, the absence of other key species in the reaction mixture can lead to various degrees of uncertainty in the applicability of model compound studies with idealized catalyst surfaces to the actual system. Transient response methods where all surface and gas-phase species are simultaneously monitored in real-time provide a more robust approach for deciphering the kinetics and mechanisms of these complex systems [126–130].

Many examples can be cited from the literature where the products produced from gas-phase catalyzed reactions result in complex, multi-component mixtures containing a spectrum of both organic and inorganic products. Two examples will be provided here to illustrate some of the key challenges associated with monitoring the transient responses of the gas-phase species using quadrupole mass spectrometry, which is the primary analytical detector in the TAP reactor system.

Consider first the partial oxidation of various C_4 hydrocarbons, such as *n*-butane, *iso*-butane, *iso*-butylene, 1-butene, 2-butene, or 1,3-butadiene to various organic ethers, ketones, aldehydes, and carboxylic acids over various metal oxide catalysts. Fig. 8 shows some of the reaction pathways and the associated products that can be produced through the selective abstraction of hydrogen or the addition of oxygen to various starting reactants and reactive intermediates. It is evident that a variety of isomers and other derivatives can be produced depending upon the dominant reaction pathway.

Reaction intermediates and products that have been reported in the catalyst literature when either *n*-butane, various butylenes, or butadiene are used as the carbon source over various metal oxide catalysts include 1-butene, 2-butene, butadiene, acetone, methyl ethyl ketone, methyl vinyl ketone, furan, dihydrofuran, maleic anhydride, acetic acid, crotonic acid, acrylic acid, glyoxylic acid, methacrylic acid, formaldehyde, acetaldehyde, propionaldehyde, crotonaldehyde, methacrolein, carbon oxides, and water [131]. Identification and quantification of the products generated from these C_4 hydrocarbons using steady-state and transient response experiments poses a significant challenge for any on-line analytical system because of the variety of reaction products that can exist under various reaction conditions and the common molecular functionalities between the various species. In the case of packed-bed microreactor systems used for catalyst screening and kinetic evaluation for *n*-butane oxidation, such as the multiple automated reactor system (MARS) [132–134], special-purpose multi-dimensional gas chromatographic methods have been developed to resolve and identify all of the C_1 to C_4 hydrocarbons, oxygen-containing organic species, and inorganic products [131]. This suggests that special methods may be needed when performing single ion monitoring of selected species to obtain reliable transient response data for reacting systems involving a complex distribution of reaction products.

Fig. 9 is a matrix that shows typical molecules that have been identified in reaction mixtures for the partial oxidation of *n*-butane to maleic anhydride over vanadium–phosphorus oxide catalysts under oxygen-rich conditions as encountered in fixed-bed processes [135,141]. The organic products include acetic acid, furan, dihydrofuran, acrylic acid, and maleic anhydride along with various C_4 hydrocarbons, CO_x, and H_2O. Selected ions produced from electron-impact ionization of each species are also listed to illustrate complexities that can occur if single-ion monitoring is performed. Other ions are also produced but are not listed for brevity. For a given hydrocarbon or organic oxygen-containing specie, several common ions occur so that the response for a particular ion would represent the combined response from several species. Data handling methods for quantifying multiple ion responses that account for these effects are well-known in

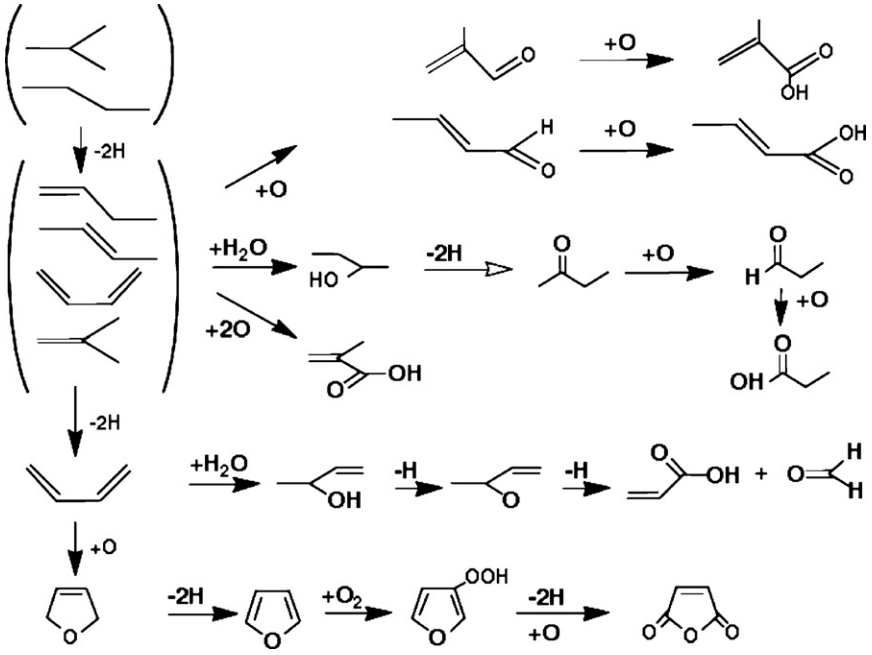

Fig. 8. Reaction pathways and products that can be generated from the selective oxidation of various C_4 hydrocarbons over metal oxide catalysts.

Species	18	25	26	27	28	29	32	38	39	41	42	43	44	45	53	54	55	56	58	60	68	70	72	98
H_2O	x																							
N_2					x																			
CO					x																			
O_2							x																	
CO_2					x								x											
Butadiene				x					x						x	x								
1-butene									x	x							x	x						
2-butene									x	x						x	x	x						
n-butane					x	x				x		x							x					
Acetic acid						x						x		x						x				
Furan						x		x	x												x			
dihydrofuran									x	x	x											x		
Acrylic acid			x	x													x						x	
Maleic anhydride		x	x		x											x								x

Fig. 9. List of species identified from GC/MS analysis of reaction products from the partial oxidation of *n*-butane over a vanadium–phosphorus oxide catalyst [134]. The indicated ions for a given species are a subset of all the ions that can be generated to illustrate the overlap that can occur. The first row in the table indicates the mass to charge ratio (m/z) of the species.

the mass spectrometry literature, which are often based upon the implementation of convolution methods [136]. However, one complication that can occur when applying these to TAP data is that transient experiments must be repeated at different ions before a composite set of ion response versus time data can be assembled. This requires that the initial state of the catalyst can be reproduced within a tolerable level of error so that the resulting responses are representative of the same surface reactions that occurred in each of the preceding set of experiments where the responses of different ions were measured. This is particularly important for many catalysts where the surface coverage, oxidation state, active sites, etc. can undergo significant changes when exposed to small doses of one or more species. Unless the composition of the reaction products can be determined *a priori* through some independent means, such as GC/MS or from previous experience with the same catalyst system, caution must be exercised to ensure that the resolution and quantification of the primary reactants and products, *i.e.*, *n*-butane, oxygen, maleic anhydride, carbon oxides, and water, is not corrupted by the presence of one or more unidentified species.

Simultaneous measurement of both gas-phase and surface species during the course of various TAP reactor transient response experiments for complex, multi-component catalytic reactions is one of the outstanding opportunities associated with strengthening, advancing, and broadening the utility of the technique. This section summarizes some recent advances in coupling analytical techniques to the TAP reactor as part of a larger effort to perform qualitative identification and quantitative analysis for the gas-phase species that are produced during the course of a single transient response experiment. The particular methods described here include: (1) time-of-flight (TOF) mass spectrometry with electron-impact (EI) ionization, and (2) on-line gas chromatography with mass spectrometry (GC/MS) where gas samples are introduced to the GC column by capturing a small (250 μl) gas sample of the transient response at various times along the response trajectory. The primary objective here is to illustrate the basic features for these systems, and to briefly demonstrate their utility for studying heterogeneous catalysis behavior using the TAP reactor system.

4.2. TAP reactor—time-of-flight system

This section summarizes the key results from a prototype system that was developed to demonstrate the feasibility of coupling a TAP reactor to a time-of-flight (TOF) mass spectrometer system for simultaneous monitoring of multiple ions from a single pulse or other type of input. A quadrupole mass spectrometer (QMS) was also included in the system to provide an independent source of data for single ion monitoring.

4.2.1. System description

A schematic of the prototype system that was developed to test coupling of a TAP microreactor to a TOF mass spectrometer is shown in Fig. 10. A simplified vacuum system was developed that allowed the TOF analytical package to be readily coupled to a TAP microreactor that was fitted with a set of high-speed pulse valves. Referring to Fig. 10, the system contains a single 20 cm vacuum chamber in which the TAP fixed-bed microreactor and pulse valves are mounted in a vertical orientation in the center of the top plate. The microreactor and pulse-valve manifold are located on the top of the vacuum chamber for ease of operation and maintenance. The reactor can be isolated from the primary chamber using a custom-designed flange valve. A quadrupole mass spectrometer (UTI, Model 100C) is mounted on a 12 cm flange so the ionization cage is perpendicular to the flight of the reactor product gas. This provides a secondary source of ion monitoring in addition to the TOF multiple ion monitoring comparison of the reactor responses. A linear time-of-flight (TOF) mass spectrometer (Jordan TOF Products, Grass Valley, CA) is connected to the main vacuum chamber in a horizontal orientation using a six-inch flange. The flight tube has an overall length of ca. 91 cm that terminates with a microchannel plate (MCP) detector. The electron gun for the TOF system is

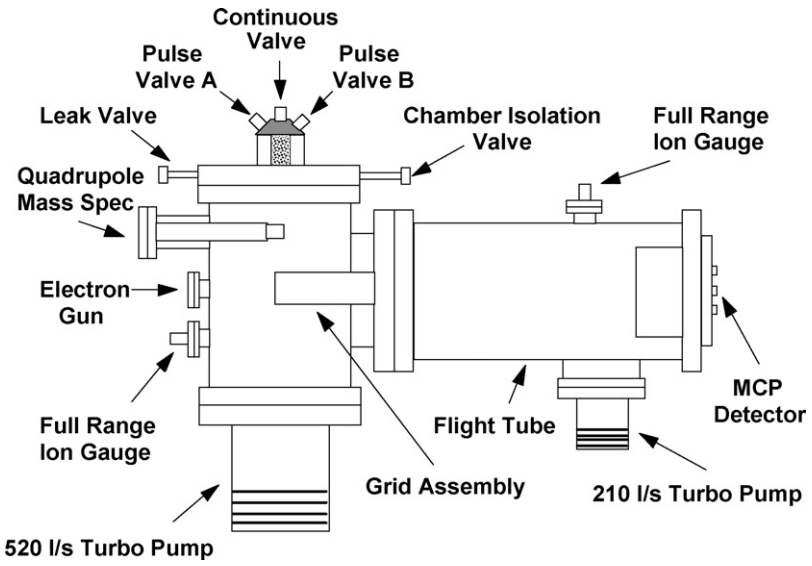

Fig. 10. Schematic of a TAP reactor coupled to a time-of-flight mass spectrometer.

mounted on a 7 cm flange directly across from the flight tube grid assembly. To monitor the pressure in main vacuum chamber and the flight tube, full-range ion gauges are mounted on two 2 cm flanges. Vacuum in the primary chamber is provided by a 520 l/s turbo molecular pump, while additional vacuum for the TOF flight tube is provided by a 210 l/s turbo molecular pump. With this combination of pumps, a background pressure of ca. 10^{-6} Pa is achieved in the flight tube, while 10^{-5} Pa is obtained in the primary chamber.

The fixed-bed TAP microreactor is constructed of type 316 stainless steel and has an inner diameter of 5.5 mm with an overall length of 41.7 mm. It seals against the heated valve manifold using a Kalrez® O-ring (DuPont Performance Elastomers, Wilmington, DE). A custom-designed splitter valve for directing a continuous controlled leak of the reactor product gas to the vacuum chamber can also be attached to the reactor exit. The reactor is packed by sandwiching the catalyst particles between two sections of 250–425 μm quartz beads. The front inert section serves to preheat the inlet gas, while the post-inert section minimizes the dead volume and broadening of the response once the product gas exits the catalytic section.

4.2.2. TOF operation and data collection

The basic design concept of the TOF spectrometer, when used as a detector for TAP reactor transient response experiment with electron-impact ionization, is illustrated in Fig. 11. The basic principles and operation of the TOF are generally described by Cotter [137] so they are omitted here. The molecular beam generated from the TAP is introduced to the ionization zone which initiates the various processes needed to create a product signal from the microchannel plate detector (MCP). The design shown in Fig. 11 is a linear TOF, although the current version in our lab employs an angular reflectron (AREF) TOF for higher mass resolution. Because the TOF system was being evaluated for the first time as a new technique for collection of time-resolved transient kinetic data from a heterogeneous catalyzed reaction, a special-purpose control and data acquisition system was developed using commercially available components.

The TOF spectrometer is typically calibrated by injecting a gas mixture containing He, Ne, N_2, Ar, and CO_2, Xe, and other components using the TAP reactor pulse-valve manifold and measuring the time-of-flight of the detected ions. These gases are selected to span the range of molecular weights that are typically encountered in TAP reactor applications, such as those involving the partial oxidation of light hydrocarbons. The flight time for CO_2 is about 10 μs so that a complete product gas mass spectrum for typical gas-phase heterogeneous reactions can be typically collected in about 30–40 μs. By contrast, the time required for the UTI quadrupole to scan over the same range, assuming 4 points per amu, would be a few seconds. The TOF clearly permits rapid detection of multiple

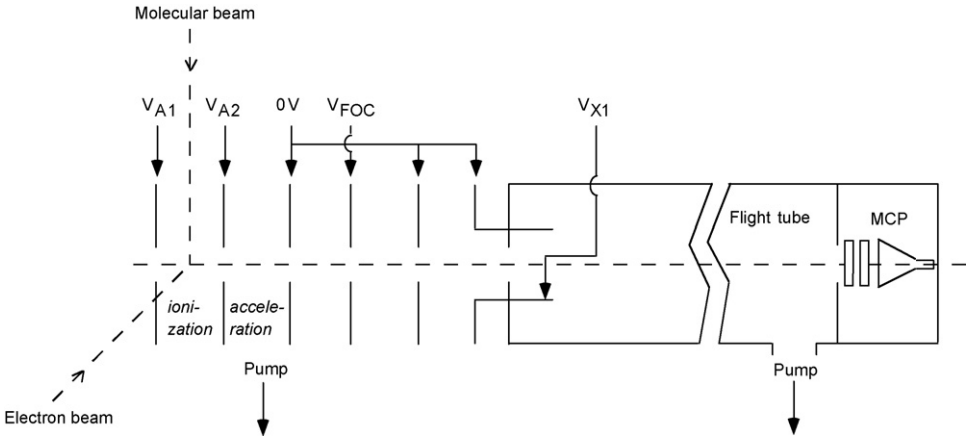

Fig. 11. Linear time-of-flight mass spectrometer. V_{A1} = repeller plate voltage, V_{A2} = extraction grid voltage, V_{FOC} = focusing voltage, V_{X1} = beam steering voltage and MCP = microchannel plate detector.

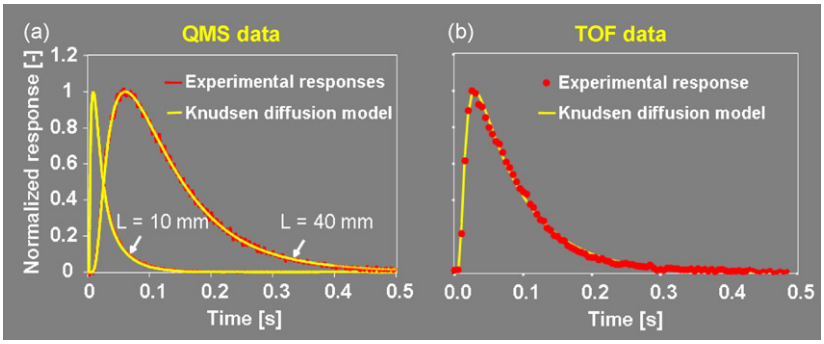

Fig. 12. Comparison of experimental and model-predicted responses obtained when the TAP–TOF system is operated using the QMS and TOF detectors. (a) QMS detector; pulsed gas = He; packing = SiC granules; particle density ρ_p = 3.2 g/cc; particle diameter d_p = 175 μm; reactor inner diameter d_r = 5.5 mm; T = 25 °C; packing length L = 10 mm (case 1) and 40 mm (case 2). (b) TOF detector; pulsed gas = CO_2; packing = quartz granules; particle density ρ_p = 2.6 g/cc; particle diameter d_p = 338 μm; reactor inner diameter d_r = 5.5 mm; T = 25 °C; packing length L = 40 mm.

ions from a single pulse input at a rate that is several orders-of-magnitude faster when compared to the QMS.

4.2.3. Example application: simultaneous collection of multiple ion spectra

Fig. 12 compares the experimental and model-predicted responses obtained when a Knudsen diffusion model discussed in a later section is used to fit TAP vacuum response data measured using the QMS and TOF detectors in separate experiments using inert gases and inert packing. The experimental details are provided in the figure caption. The results show that both the QMS and TOF experimental responses are in good agreement with the predictions of the single parameter Knudsen diffusion model. This provides verification that the responses are not affected by the vacuum system design or other related instrument-related parameters. Additional details on the time-of-flight system design in connection with the TAP reactor and its application are omitted here for brevity but will be provided in future publications from our group.

The validity of the TAP reactor responses measured by the TOF in Fig. 12, as well as the response data measured by the QMS, can be evaluated by comparing ratios of the Knudsen diffusion coefficients to the ratio of the inverse square root of their molecular weights in accordance with the theoretical expression for the Knudsen diffusion coefficient based upon the kinetic theory of gases. The Knudsen diffusion coefficients were obtained by fitting the experimental responses to the model-predicted experimental response. The results of this analysis are shown in Fig. 13. The data for He was used as the reference gas, although the use of other species for the reference had a negligible effect. The data generate a response whose slope is unity, which should be the case if Knudsen diffusion is the primary mode of gas transport and instrument effects are negligible.

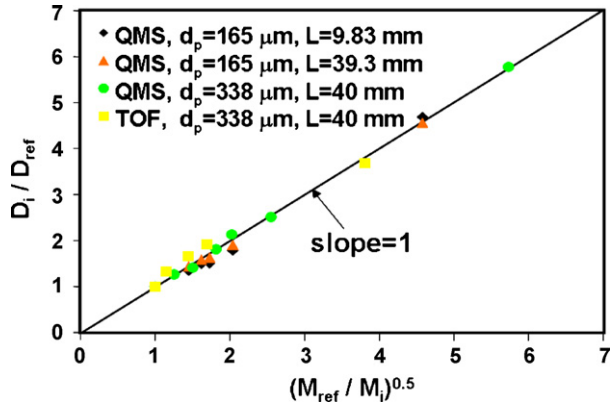

Fig. 13. Test of the experimental response data fitted to the single parameter Knudsen diffusion model using data generated from both the TOF and QMS detectors.

4.3. TAP reactor with on-line GC/MS system

TAP reactor transient response experiments that produce reaction products with complex mass spectrometer fragmentation patterns from the quadrupole mass spectrometer detector require development of special experimental methods and signal processing techniques before the response of a particular species can be extracted from the ion response versus time matrix. Analysis of the product gas composition along the transient response trajectory represents key information that is needed for modeling of the transport-kinetic interactions that describe the TAP reactor performance. When a time-of-flight mass spectrometer is used instead of a quadrupole mass spectrometer, the ion response versus time matrix can be assembled from the data generated by the TOF microchannel plate detector during the passage of a single pulse input or other user-defined sequence of pulse inputs, e.g., multi-pulse or pump-probe inputs. Conversion of the raw ion response versus time matrix to the species concentration versus time matrix first requires qualitative identification of all species in the mixture. Once this is accomplished, response factors for the individual ions of a given species can be assigned so that the measured response of a given ion can be used to compute the instantaneous gas composition using standard data modeling methods, such as AMDIS [138].

Special-purpose hardware interfaces have been developed to generate step-up or step-down concentration inputs to a TAP-1 microreactor system [16,19,20] operating with a continuous gas flow at atmospheric pressure. The reactor product gases can be routed through a low dead volume heated gas leak valve and transfer line so that the transient responses can be sampled on-line and analyzed using a GC/MS system. The time at which a gas sample is captured is user-defined and can be any point along the trajectory of the transient response. In addition, a small (<0.5 sccm), controlled continuous leak of the product gas can be directed to the TAP analytical chamber that houses the quadrupole, thereby allowing for continuous monitoring of a single ion. The technique could be readily extended to the case when a TOF is used, thereby providing simultaneous monitoring of all key ions and their subsequent specie assignments using data from the GC/MS system.

Although the experimental methodology was initially demonstrated using a TAP-1 system, the approach used here for capturing the on-line gas sample for subsequent GC/MS analysis could be readily adapted to the TAP-2 [14] and future system designs. It could also be adapted for product analysis from TAP pulsed high-vacuum experiments for product identification and quantification,

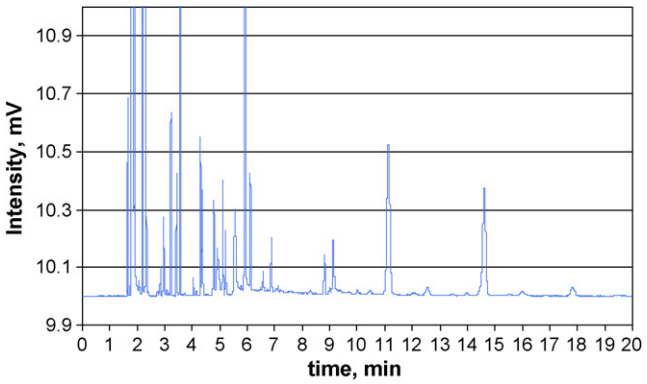

Fig. 14. Chromatogram from FID analysis of a product mixture from a typical steady-state catalyst test for the partial oxidation of 1,3-butadiene to furan. Reactor feed composition: 8.8% 1,3-butadiene, 10.3% oxygen, 9.0% nitrogen and balance: helium; reaction temperature: 380 °C. GC column: 0.53 mm i.d. × 30 m 1701 phase, film thickness = 5 μm.

which represents a departure from dedicated step-response reactor systems designed for dedicated operation at normal pressures. Addition of a GC/MS is particularly useful since the various species present in the product gas mixture are first resolved into component peaks using an appropriate arrangement of GC columns using either a flame ionization or thermal conductivity detector with a small continuous split gas flow being directed to the mass spectrometer. The GC peaks are assigned to a unique species by matching the ionization fragmentation patterns using standard mass spectrum library software, such as the Wiley NIST/EPA/NIH library [158].

4.3.1. Example application: oxidation of 1,3-butadiene over a $CuBi_bPb_cMo_dO_x$ catalyst

Fig. 14 shows the chromatogram produced from analysis of the product mixture from steady-state TAP reactor continuous-flow experiments at atmospheric pressure for the partial oxidation of 1,3-butadiene to furan over a $Cu_{0.2}Bi_{1.95}Pb_{0.05}MoO_6$ catalyst at 380 °C. This particular catalyst is a member of a family of modified Pb–Bi–Mo_xO_y catalysts containing vanadium, copper, or gold, and is useful for the gas-phase oxidation of an unsaturated acyclic hydrocarbon with selectivity to the corresponding furan product [99,159]. Other experimental particulars are provided in the figure caption. This example was selected to illustrate the analytical complexity that can be encountered during the catalyst discovery stage, and to illustrate the utility of an on-line GC/MS for species identification when integrated into the TAP system configuration. The product gas sample was captured on-line using a multi-port gas sampling valve, and was transferred directly to the inlet of an Agilent 6890 GC equipped with both a FID and an Agilent 5973 mass selective detector through microcapillary tubing. This same product distribution was also independently reproduced in a MARS reactor [132] for validation of the TAP system setup.

The organic products that were positively identified in the product gas matrix are shown in Fig. 15, which accounts for more than 80% of the total number of peaks. Inspection of the indicated compounds provides initial insight into the complexities of the catalytic mechanisms and reaction pathways that must be operative for some of these to be produced, particularly the functionalized aromatics, cyclic ethers, and organic acids. A more in-depth interpretation of the catalytic chemistry is not included here, but is a topic of ongoing research. However, this product distribution points to the complexities that will occur when single or multiple ion monitoring is used to detect the transient behavior of a particular reactant or product. This suggests that identification of the transient responses of various species will require data processing methods

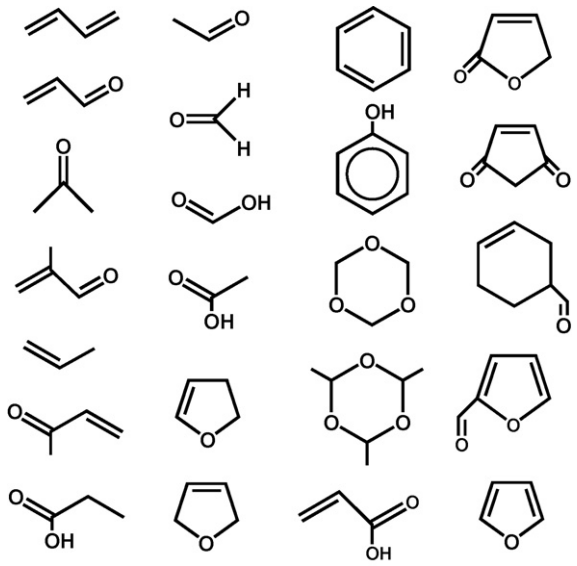

Fig. 15. Structures of the organic products identified in the product gas for the partial oxidation of 1,3-butadiene to furan. Reactor feed composition: 8.8% 1,3-butadiene, 10.3% oxygen, 9.0% nitrogen and balance: helium; reaction temperature: 380 °C.

for deconvolution of the product spectrum, which must be incorporated into future TAP reactor systems that have multi-functional capabilities.

4.3.2. Closing comments

Catalytic reactions that produce a distribution of products require identification of the major species that are present before any detailed study of the transient kinetics can be conducted. Advanced analytical methods, such as time-of-flight mass spectrometry and GC/MS, are both useful for both qualitative identification and quantitative analysis when coupled to the existing TAP quadrupole mass spectrometer system. Future TAP applications will require the use of more sophisticated analytical methods to obtain quantitative information on the interaction between gas-phase and surface-catalyzed processes.

5. Theory of TAP packed-bed microreactor configurations

The analysis of TAP pulse-response experiments are based on specific microreactor models that describe the catalyst zone. Current models apply to packed-bed reactors, starting with a one-zone reactor, and progressing to a reactor containing a single particle [17,18]. When the input pulse intensity is $\approx 10^{14}$ molecules/pulse transport in the reactor is dominated by Knudsen diffusion, which is mainly driven by a gas concentration gradient. The magnitude of the gradient is dependent on the reactor length and the vacuum boundary condition at the reactor outlet. Under the conditions of catalytic reaction, the gas concentration gradient causes a surface concentration gradient in the catalyst bed. When the length of the catalyst bed is a significant fraction of the reactor length, the reactant can cause non-uniformity in the catalyst composition [109–112].

TAP microreactor development has focused on minimizing the effects of temperature and concentration gradients. An axial temperature gradient exists because of the close proximity of the microreactor outlet to the vacuum chamber. Typically the temperature near the center of a microreactor will be higher than the temperature close to the microreactor outlet. The evolution of TAP microreactor configurations and their theoretical description will be presented in the following sections.

5.1. Basic concepts

There are three basic concepts that form the basis for extracting kinetic information from TAP Knudsen pulse-response experiments:

1. Well-defined Knudsen diffusion is a "measuring stick" for measuring chemical reaction rates and extracting kinetic parameters.
2. During a single pulse experiment the solid catalyst changes insignificantly and controlled change occurs in a multi-pulse experiment.
3. The solid catalyst surface composition will remain uniform if the active zone is a sufficiently small fraction of the total bed length.

The first and second concepts were reported implicitly in the first TAP paper in 1988 [16]. In the 1997 TAP paper [14], the above concepts were expressed explicitly and presented mathematically. The concept of uniformity was stressed in the paper devoted to the thin-zone TAP reactor in 1999 [109].

5.1.1. Knudsen diffusion as a "measuring stick"

Since Temkin's [143–145] and Denbigh's [146,147] times, a common approach for extracting kinetic information is to measure the rate of chemical reaction using the rate of mass transport as a "measuring stick." In traditional steady-state experiments with perfect mixing, convectional transport is the "measuring stick" and diffusional transport is neglected. In TAP Knudsen pulse-response experiments there is no convective flow and Knudsen diffusion is the only gas transport process. In the absence of reaction, the gas exit flow from the microreactor is described by a standard diffusion curve. In the "reaction-diffusion" case, the exit flow response curve is different from the standard diffusion curve, and this difference is attributed to reaction.

5.1.2. Insignificant change in the solid catalyst during single pulse experiment and controlled change during multi-pulse experiments

When the number of reactant gas molecules in a single pulse is significantly smaller than the number of catalytically active sites on the catalyst, the catalytic system remains in essentially the same state after the measurement. This type of experiment is called a "state-defining" experiment [14]. A series of state-defining experiments can cause the catalyst state to change, and the change is characterized by the amount of consumed/released gaseous substances. A series of state-defining experiments is termed a "state-altering" experiment [14].

5.1.3. Uniformity of the catalyst surface composition across the active zone

When a heterogeneous catalyst is exposed to a reactant gas the composition and kinetic properties of the catalyst can change as a result of reaction with the gas. In a packed-bed reactor, the gas flow can cause the change to occur non-uniformly. The inlet of the bed will see the highest reactant concentration, and will change by the largest amount. In a non-steady-state experiment the bed composition can also change in time. An important and unique feature of a TAP pulse-response experiment is that the catalyst composition remains essentially uniform when the thickness of the catalyst zone is small compared to the total length of the packed bed. In practice a small amount of catalyst can be packed in a "thin zone" between two beds of inert particles or in some cases a single particle can be used. The advantage and properties of a thin-zone TAP reactor (TZTR) have been discussed in detail in the literature [33,109–112,148]. The properties of a single particle TAP reactor [17,18] have recently been described.

Using a TZTR, a catalyst sample can be characterized "state-by-state" to determine how its catalytic properties change as a result of reaction. This process has been demonstrated using the selective oxidation of hydrocarbons over a transition metal oxide catalyst (e.g., vanadyl pyrophosphate or VPO) [33,140]. An oxidized VPO sample was exposed to a series of hydrocarbon pulses and the change in kinetic properties were determined as a function of the oxidation degree.

5.1.4. TAP studies and model-free kinetic analysis

The goal of model-free kinetic analysis is to obtain the rate of chemical transformation without assuming a specific kinetic model. Temkin and Denbigh applied a model-free approach to the analysis of steady-state kinetics for over 50 years. In their approach, the rate of chemical substance transformation is equal to the difference between the inlet and outlet molar flow rates divided by the catalyst volume or surface area. In CSTR steady-state experiments no assumptions regarding the type of kinetic dependence, the reaction mechanism, or the corresponding model are needed to determine the rate of chemical transformation. Model-free kinetic analysis of non-steady-state reactions [148] is a recent development that began with the TZTR microreactor configuration.

A model-free kinetic method known as the "Y-procedure" [148] has been used to extract the non-steady-state rate of chemical transformation from reaction-diffusion data with no assumptions regarding the kinetic model. This method will be briefly described in a separate section of this paper. The Y-procedure consists of the following steps:

1. Exact solution in the Laplace domain.
2. Switching to the Fourier domain to allow sufficient computation.
3. Introduction of discretization and filtering in the Fourier domain to deal with real data (in the time domain) subject to noise.

Overall, the methodology used in TAP Knudsen pulse-response experiments combines experimental conditions that simplify the physico-chemical system with basic mathematical ideas—especially with the idea of infinitesimal change.

5.2. One-zone TAP microreactor

In the one-zone microreactor model the total reactor volume is uniformly packed with catalyst particles. The one-zone model and its mathematical framework were introduced in the first TAP paper published in 1988 [16]. The mathematical model is based on the following assumptions:

1. The fractional voidage of the catalyst bed is constant.
2. There is no radial concentration gradient in the catalyst zone.
3. There is no radial or axial temperature gradient in the catalyst zone.
4. There is no intra-particle or surface diffusion.
5. The diffusivity of each gas is constant and independent of the composition of the mixture as a whole.

The last assumption results from using an evacuated microreactor and small pulse intensities, which guarantees the validity of the Knudsen diffusion regime. The mass balance equations for a number of important gas transport and transport-kinetics interactions in the one-zone reactor are presented below.

5.2.1. Diffusion only

In a packed-bed reactor, the mass balance equation for Knudsen diffusion of a non-reacting gas A (e.g., neon, argon and krypton) is given by

$$\varepsilon_b \frac{\partial C_A}{\partial t} = D_{eA} \frac{\partial^2 C_A}{\partial z^2}, \quad (1)$$

with initial condition:

$$0 \le z \le L, \quad t = 0, \quad C_A = \delta_z \frac{N_{pA}}{\varepsilon_b A}, \tag{2}$$

and boundary conditions:

$$z = 0, \quad \frac{\partial C_A}{\partial z} = 0, \tag{3}$$

$$z = L, \quad C_A = 0. \tag{4}$$

The initial condition, Eq. (2), specifies that at $t = 0$, the gas concentration at the reactor inlet can be represented by the delta function. Boundary condition one, Eq. (3), specifies that the input flux is zero at the microreactor entrance when the pulse-valve is closed. Boundary condition two, Eq. (4), specifies that the gas concentration at the microreactor outlet is very close to zero. This condition results from the continuous evacuation of the microreactor outlet by the vacuum system. The diffusivity term in the Knudsen diffusion regime is determined by the following equation [32]:

$$D_e = \frac{\varepsilon_b}{\tau}\frac{d_i}{3}\sqrt{\frac{8RT}{\pi M}}, \quad d_i = \frac{4\varepsilon_b}{3(1-\varepsilon_b)}r_p. \tag{5}$$

The flow rate, F_A, at the microreactor outlet is described by the following equation:

$$F_A = -AD_{eA}\frac{\partial C_A}{\partial z}\Big|, \tag{6}$$

and the gas flux by

$$Flux_A = \frac{F_A}{A}. \tag{7}$$

In order to solve for the gas exit flow rate, it is useful to express Eq. (1) in dimensionless form:

$$\bar{F}_A = \pi\sum_{n=0}^{\infty}(-1)^n(2n+1)\ \exp(-(n+0.5)^2\pi^2\tau). \tag{8}$$

Eq. (8) describes the dimensionless exit flow rate as a function of dimensionless time. The resulting curve (Fig. 16) is known as the standard diffusion curve. For any TAP vacuum pulse-response experiment that involves only gas transport, the standard diffusion curve should be the same regardless of the gas, microreactor bed length, catalyst particle size, or reactor temperature. The area under the standard diffusion curve is to equal unity. In dimensional form, Eq. (8) can be rewritten as

$$\frac{F_A}{N_{pA}} = \frac{D_{eA}\pi}{\varepsilon_b L^2}\sum_{n=0}^{\infty}(-1)^n(2n+1)\ \exp(-(n+0.5)^2\pi^2\frac{tD_{eA}}{\varepsilon_b L^2}). \tag{9}$$

Eq. (9) indicates that the pulse shape of the curve generated in a diffusion only experiment should be independent of the pulse intensity if the gas molecules are transported through the microreactor in the Knudsen diffusion regime.

A unique feature of the standard diffusion curve is the time, τ_p, at which the curve maximum occurs is given by

$$\tau_p = \frac{1}{6}, \tag{10}$$

and the corresponding height of the peak maximum is given by

$$\bar{F}_{A,p} = 1.85. \tag{11}$$

Eqs. (10) and (11) can be rewritten in dimensional form in terms of time and height as

$$t_p = \frac{1}{6}\frac{\varepsilon_b L^2}{D_{eA}}, \tag{12}$$

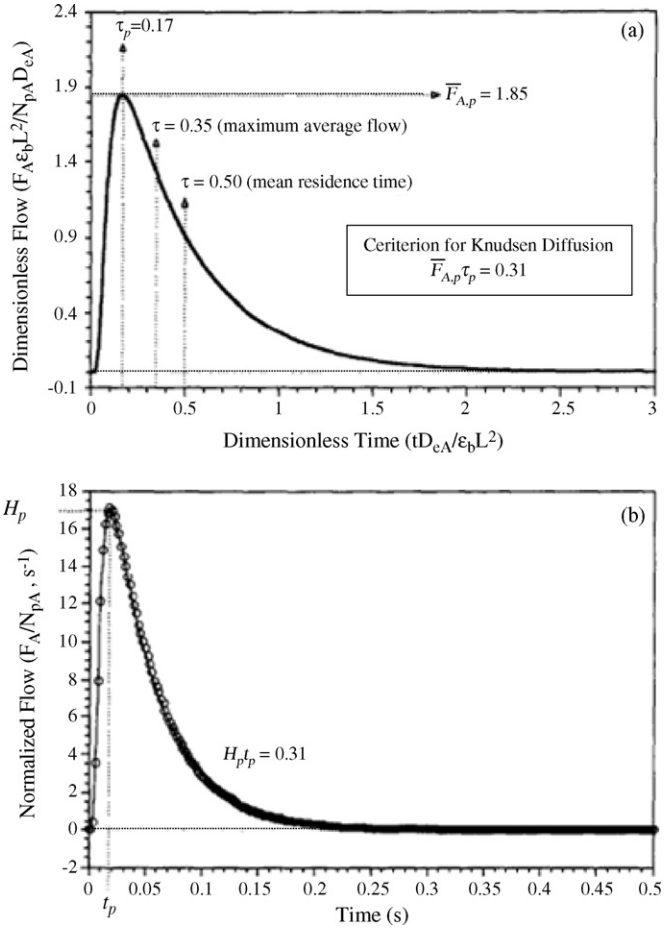

Fig. 16. (a) Standard diffusion curve showing key time characteristics and the criterion for Knudsen diffusion. (b) Comparison of standard diffusion curve with experimental inert gas curve over inert packed bed [14].

and

$$H_p = 1.85\frac{D_{eA}}{\varepsilon_b L^2}. \tag{13}$$

By multiplying Eq. (10) with (11) and Eq. (12) with (13) gives a relationship between the time at which the peak maximum occurs on a standard diffusion curve and its corresponding peak height. This calculation can be used to verify that gas transport through the reactor is Knudsen diffusion:

$$\bar{F}_{A,p}\tau_p = t_p H_p \approx 0.31. \tag{14}$$

5.2.2. Diffusion + irreversible adsorption/reaction

If adsorption or reaction is first order in gas concentration, and surface coverage is negligible (the result of small pulse intensity) compared to the total amount of active catalytic material, then the mass balance for the gas-phase component A is given by Eq. (15):

$$\varepsilon_b\frac{\partial C_A}{\partial \tau} = D_{eA}\frac{\partial^2 C_A}{\partial z^2} - a_s S_v(1-\varepsilon_b)k_a C_A, \tag{15}$$

which can also be written in dimensionless form:

$$\frac{\partial \bar{C}_A}{\partial \tau} = \frac{\partial^2 \bar{C}_A}{\partial \zeta^2} - \bar{k}_a\bar{C}_A, \quad \bar{k}_a = \frac{a_s S_v(1-\varepsilon_b)k_a L^2}{D_{eA}}. \tag{16}$$

The dimensionless exit flow rate for irreversible adsorption or reaction combined with Knudsen diffusion process is given by

$$\bar{F}_A = \pi\ \exp(-\bar{k}_a\tau)\sum_{n=0}^{\infty}(-1)^n(2n+1)\ \exp(-(n+0.5)^2\pi^2\tau), \tag{17}$$

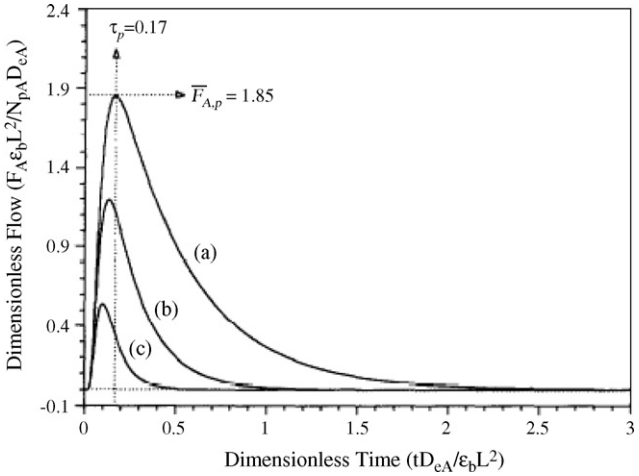

Fig. 17. Comparison of diffusion + irreversible adsorption/reaction exit-flow curves with the standard diffusion curve. (a) Standard diffusion exit-flow curve, $\bar{k}_a = 0$, (b) diffusion + irreversible adsorption/reaction curve, $\bar{k}_a = 3$ and (c) diffusion + irreversible adsorption/reaction curve, $\bar{k}_a = 10$.

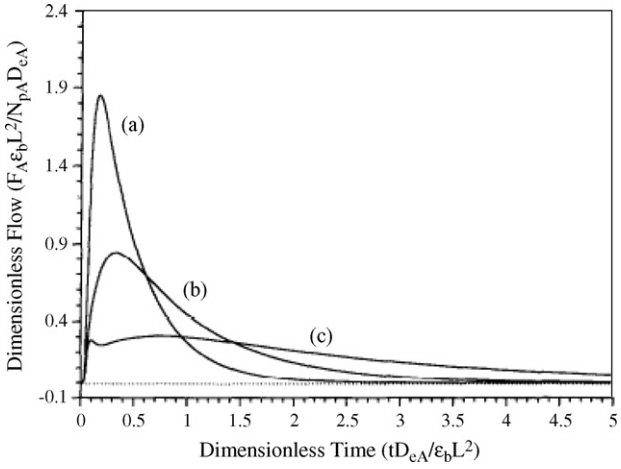

Fig. 18. Comparison of standard diffusion and diffusion + reversible adsorption exit-flow curves. (a) Standard diffusion exit-flow curve, $\bar{k}_a = 0$, (b) diffusion + reversible adsorption curve, $\bar{k}_a = 20$, $\bar{k}_d = 20$ and (c) diffusion + reversible adsorption curve, $\bar{k}_a = 20$, $\bar{k}_d = 5$[14].

Eq. (17) can also be written in dimensional form as

$$\frac{F_A}{N_{pA}} = \frac{D_{eA}\pi}{\varepsilon_b L^2}\ \exp(-k'_a t)\sum_{n=a}^{\infty}(-1)^n(2n+1) \times \exp\left(-(n+0.5)^2\pi^2\frac{D_{eA}}{\varepsilon_b L^2}\right), \quad (18)$$

where

$$k'_a = \frac{a_s S_v(1-\varepsilon_b)k_a}{\varepsilon_b}. \quad (19)$$

A comparison between the dimensional forms of the exit flow for the irreversible adsorption/reaction case, Eq. (18), and the standard diffusion curve, Eq. (9), shows that the values of the normalized exit flow for irreversible adsorption/reaction is less than the values obtained in the diffusion only case by a factor of $\exp(-k'_a t)$. Therefore, the normalized exit-flow curve versus time for irreversible adsorption/reaction is always smaller than the standard diffusion curve (Fig. 17). Accurate extraction of kinetic constants based on comparison with the standard diffusion curve is possible only in a special domain of parameters. Time of reaction cannot be too fast or too slow in comparison with transport residence time. A special analysis of this domain is in the literature [156,157].

5.2.3. Diffusion + reversible adsorption

When diffusion + reversible adsorption occurs, and the number of gas molecules is small compared to the total number of catalytically active sites, the mass balances of component A in the gas phase, and on the catalyst surface are described respectively by the following two equations:

$$\varepsilon_b\frac{\partial C_A}{\partial t} = D_{eA}\frac{\partial^2 C_A}{\partial z^2} - a_s S_v(1-\varepsilon_b)(k_a C_A - k_d\theta_A), \quad (20)$$

$$\frac{\partial\theta_A}{\partial t} = k_a C_A - k_d\theta_A. \quad (21)$$

The dimensionless desorption rate constant is defined as

$$\bar{k}_d = k_d\frac{\varepsilon_b L^2}{D_{eA}}. \quad (22)$$

Eqs. (20) and (21) can be rewritten in dimensionless form as

$$\frac{\partial\bar{C}_A}{\partial\tau} = \frac{\partial^2\bar{C}_A}{\partial\zeta^2} - \bar{k}_a\bar{C}_A + \bar{k}_d\bar{\theta}_A, \quad (23)$$

$$\frac{\partial\bar{\theta}_A}{\partial\tau} = \bar{k}_a\bar{C}_A - \bar{k}_d\bar{\theta}_A, \quad (24)$$

where

$$\bar{\theta}_A = \alpha\theta_A, \quad (25)$$

and

$$\alpha = (1-\varepsilon_b)AL\frac{a_s S_v}{N_{pA}}. \quad (26)$$

Eqs. (23) and (24) can be solved using the dimensionless initial and boundary conditions for the diffusion only process with the additional initial condition for the coverage of adsorbed component A:

$$t = 0, \quad \bar{\theta}_A = 0. \quad (27)$$

The complete solutions for the dimensionless concentration and exit flow can be found in the literature [14].

In contrast to the normalized exit-flow curve in the process of diffusion + irreversible adsorption/reaction, the exit-flow curve for the diffusion + reversible adsorption crosses the standard diffusion exit-flow curve (Fig. 18).

The point at which the curves intersect depends on the adsorption and desorption rate constants. The diffusion + reversible adsorption exit-flow curve is wider and crosses the standard diffusion curve because of the time delay in molecular transport resulting from the interaction of gas molecules with the catalyst surface. The shape and magnitude of the diffusion + reversible adsorption exit-flow curve is also strongly influenced by the adsorption–desorption parameters. For example, when the adsorption rate constant is large, and the desorption rate constant is small; the exit-flow curve has two peaks [14]. The first peak resembles an irreversible adsorption exit-flow curve, and is governed by the interaction between diffusion and adsorption. The second peak is the result of slow desorption, and its shape is dependent on the parameters of adsorption, desorption, and diffusivity. Mathematical modeling of the two peaks shows that the catalyst surface coverage initially increases with time due to fast gas adsorption, then decreases at which time desorption becomes more significant [14].

5.3. Three-zone TAP microreactor

In the three-zone microreactor, the catalyst zone is sandwiched between two inert zones, and all three zones are of equal length

[14]. In the three-zone configuration the catalyst can be more easily maintained under isothermal conditions. However, the gas concentration gradient across the catalyst zone can create non-uniform surface coverage. Also, it is difficult to analyze the transcendental functions that contain the kinetic parameters that are solutions of the three-zone TAP model.

The three-zone mathematical model is the same used in the one-zone model with two additional boundary conditions between the inert and catalyst zones. The additional boundary conditions are given by

$$C_{A,zone1}|z_1 = C_{A,zone2}|z_1 , \quad (28)$$

$$C_{A,zone2}|z_2 = C_{A,zone3}|z_2 , \quad (29)$$

$$-D_{eA,zone1}\frac{\partial C_{A,zone1}}{\partial z}|z_1 = -D_{eA,zone2}\frac{\partial C_{A,zone2}}{\partial z}|z_1 , \quad (30)$$

$$-D_{eA,zone2}\frac{\partial C_{A,zone2}}{\partial z}|z_2 = -D_{eA,zone3}\frac{\partial C_{A,zone3}}{\partial z}|z_2 , \quad (31)$$

where z_1 is the axial coordinate at the end of zone 1, and z_2 is the axial coordinate at the end of zone 2. Eqs. (28)–(31) describe the continuity of the gaseous concentrations and flows inside the microreactor.

5.4. Thin-zone TAP microreactor (TZTR)

The thin-zone TAP microreactor (TZTR) model [33,109–112] is a three-zone configuration in which the thickness of the catalyst zone is made very small in comparison to the whole length of the microreactor. The advantage of the TZTR configuration is that any change in gas concentrations across the catalyst bed can be neglected when compared to their average values. Diffusional gas transport can be explicitly separated from the chemical reaction rate.

The TZTR mathematical model determines the active zone reaction rate as the difference between two diffusional flow rates at the boundaries of the thin catalyst (active) zone:

$$Rate = Flow^{left}(t) - Flow^{right}(t). \quad (32)$$

Eq. (32) is analogous to a steady-state CSTR where the reaction rate is determined by the difference between two convectional flow rates. For first-order irreversible adsorption/reaction, conversion in the TZTR can be found using:

$$X = \frac{k_{ads}\tau^{dif}_{res,cat}}{1 + k_{ads}\tau^{dif}_{res,cat}}, \quad (33)$$

where

$$\tau^{dif}_{res,cat} = \varepsilon_b \frac{(\Delta L)L_{II}}{D_{eA}}. \quad (34)$$

The apparent adsorption/reaction rate constant, k_{ads}, can be found from the relationship:

$$k_{ads} = K_a \frac{D_{eA}}{L\Delta L\varepsilon_b}, \quad (35)$$

where the dimensionless parameter K_a can be calculated from the zeroth moment:

$$\frac{1}{M_0} = 1 + K_a\frac{L_{II}}{L}. \quad (36)$$

The zeroth moment is obtained by measuring the area of a pulse response curve. Moment based analysis of TAP pulse response data is described in the literature [14,34]. Eq. (33) is analogous to the conversion expression for a first-order reaction in a CSTR:

$$X_{CSTR} = \frac{k_{CSTR}\tau^{conv}_{res}}{1 + k_{CSTR}\tau^{conv}_{res}}, \quad (37)$$

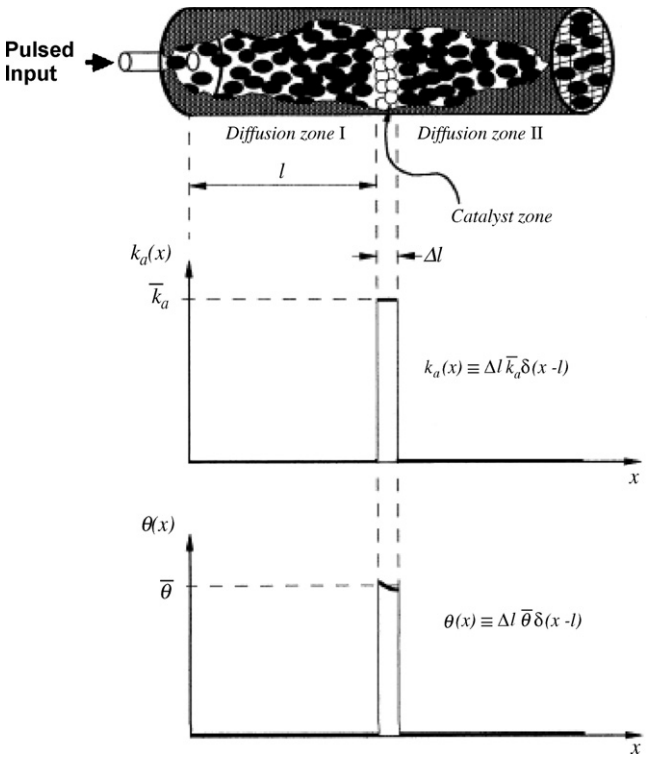

Fig. 19. Schematic representation of the thin-zone TAP microreactor and the dependencies of k_a and θ on the axial coordinate x [32].

where k_{CSTR} is the apparent rate constant, τ^{conv}_{res} is the convectional average residence time, and

$$\tau^{conv}_{res} = \frac{V_{cat}}{F_v}. \quad (38)$$

The difference between the conversion expressions for a CSTR and TZTR is that the residence time found in the TZTR, $\tau^{dif}_{res,cat}$, is proportional to the position of the catalyst zone inside the microreactor. When the catalyst zone position along the reactor axis is changed the conversion changes. For example, if it is moved closer to the microreactor inlet, conversion increases and closer to the outlet, conversion decreases. Fig. 19 shows a schematic of the TZTR and the dependence of the dimensionless adsorption constant, k_a, and the dimensionless surface coverage, θ, on the axial coordinate x.

Although concentration and temperature gradients in the catalyst zone are very small in the TZTR, some non-uniformity will still be present. Non-uniformity can be attributed to two factors: the applied concentration gradient, which drives diffusion and is present even when no reaction occurs, and chemical reaction, which changes the concentration profile in the catalyst zone [109–112]. These factors are taken into account in the following equation:

$$\frac{C_{in} - C_{out}}{C_{in}} \approx 2\frac{L_c}{L_r} + \frac{X}{1 + (1 - X)L_r/L_c}, \quad (39)$$

The first term on the right-hand side of Eq. (39) relates only to the geometric configuration of the reactor, and the second relates to the influence of chemical reaction and geometry. As with a differential PFR, non-uniformity in a TZTR is proportional to conversion, but the proportionality is not linear. Fig. 20 shows a comparison of non-uniformity in the TZTR and a PFR as a function of increasing conversion.

Over a wide range of conversions (up to 75%), the level of non-uniformity in a TZTR is not higher than 20%, and only becomes significant at conversions greater than 80%.

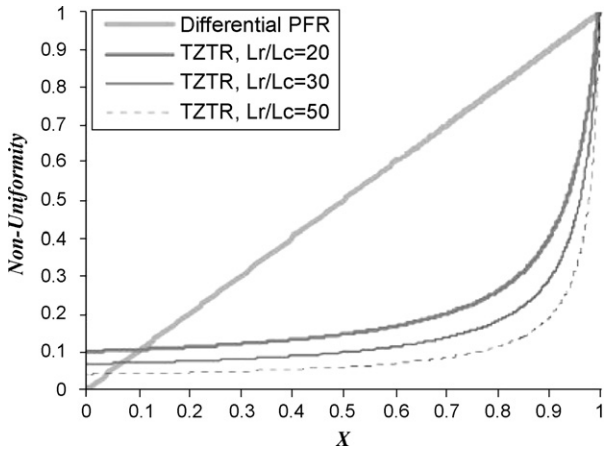

Fig. 20. Comparison of non-uniformity versus conversion for the differential PFR and TZTR. Different ratios of entire microreactor length to length of catalyst zone are given for the TZTR [109–112].

5.5. Probabilistic theory of single particle TAP experiments

The single particle experiment (see Section 6.1 for a detailed description) is the most recent addition to TAP microreactor configurations. With the single particle microreactor configuration, even higher conversions (up to 95%) can be achieved compared to the 80% conversion obtained in a TZTR to ensure uniformity in the active zone.

A two-dimensional numerical model based on probabilistic theory and interpretation of conversion based on the principle of Brownian motion of reactant molecules inside the microreactor is created to understand the trajectory and transport of reactant gas molecules in the single particle experiment.

The numerical experiment is modeled in which a pulse of gas of chemical species A is released into the microreactor and the outlet flow is collected at the right-hand side of Fig. 21. The black disc represents the catalyst particle and the light shaded dots represent the inert medium used to pack the microreactor. The black line inside the microreactor represents a possible trajectory route for a reactant gas molecule prior to exiting the microreactor.

The numerical model states that if a reactant gas molecule A remains near or comes into contact with an active catalyst particle during the course of its random motion in the packed bed of the microreactor for a certain period of time, then the probability that a reaction will occur during that time period is 1. If a reactant gas molecule A is far away from the active catalyst particle, then the probability of conversion is 0 regardless of how long gas molecule A stays in that position.

The numerical model can also determine conversion in terms of the molecular residence time in or near the active catalyst particle. If the residence time of gas molecules inside the microreactor is long, then that molecule has a high probability of spending a longer time in proximity to the active catalyst particle. Therefore, conversion of gas molecule A is likely to occur. From another standpoint, if the gas residence time in the microreactor is long, the gas molecule has a higher probability of contacting or come in close proximity to the active particle through a longer random walk before exiting the microreactor. A correlation between the numerical model and the experimental results explains that due to the high number of random gas collisions prior to exiting the microreactor, there is a greater probability for the reactant gas molecules to come into contact with the active catalyst particle and convert to the product (*i.e.*, higher conversion). Detailed results of the numerical calculations can be found in the paper [18].

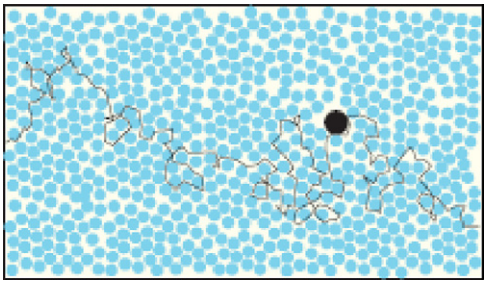

Fig. 21. Model of microreactor with catalyst (black dot) and inert quartz particles (blue dots). The dashed line at the right indicates the microreactor outlet. (For interpretation of the references to color in this figure legend, the reader is referred to the web version of the article.)

6. TAP experimental results

6.1. Bridging the pressure gap

With the TAP reactor system, a catalyst sample can be rapidly cycled between vacuum and atmospheric pressure without exposing it to the atmosphere. The process is illustrated in Fig. 22, which shows the slide valve in the high-pressure (a) and vacuum positions (b).

In the high-pressure position, the reactor effluent flows through the slide valve and out an external vent where it can be analyzed using a GC (see Section 4.3). A small portion of the effluent can be diverted to the mass spectrometer chamber, through an adjustable needle valve. The mass spectrum of the reaction products is collected in real-time. After running atmospheric pressure experiments the reactor can be evacuated, and the slide valve moved to the vacuum position. During the switch from high pressure to vacuum the reactor effluent can be monitored and desorbing adspecies left on the surface during pressure experiments can be measured. TAP pulse-response experiments are performed after the reactor reaches vacuum, and the desorption of adspecies has stopped. Switching back and forth between high-pressure and vacuum operation typically takes less than 30 s.

Recently, we reported results from atmospheric pressure and vacuum pulse-response experiments on the oxidation of CO [17]. The catalyst sample was a single 400 μm diameter polycrystalline platinum (Pt) particle, which was placed in a microreactor bed with ≈100,000 inert quartz particles with diameters between 210 and 250 μm.

Fig. 23 presents a scale drawing of the reactor configuration. The particle occupies less than 0.3% of the cross-sectional area of the microreactor, so the reaction zone can be considered a point source. Gas concentration or temperature gradients across the catalyst zone can be assumed to be negligible since the zone is a single particle.

Vacuum pulse-response experiments were performed using a "pump-probe" format illustrated in Fig. 24. Oxygen/Ar and CO/Ar mixtures are injected from different pulse valves in an alternating sequence, and the CO_2 response is measured during each pulse. Argon is used as an internal standard. CO_2 does not appear on the first oxygen pulse since no CO is present in the reactor. CO_2 appears on the first CO and all subsequent oxygen pulses.

At 170 °C the yield for the individual O_2 and CO pulses reaches a maximum, making the total yield equal to 95% during one pump-probe cycle indicating that at least 95% of CO molecules pulsed into the reactor must strike the particle. Above 170 °C the CO_2 yield decreases, more rapidly for the O_2 pulse than the CO pulse.

Atmospheric flow experiments were performed after closing the slide valve. The particle bed was first exposed to a hydrogen flow (20 cc/min diluted in Ar, H_2/Ar = 1) at 350 °C for 1 h. Hydrogen was used to remove any memory of the previous pump-probe experiments. A total flow of 50 cc/min of O_2, CO, and Ar (O_2/CO/Ar = 1) was

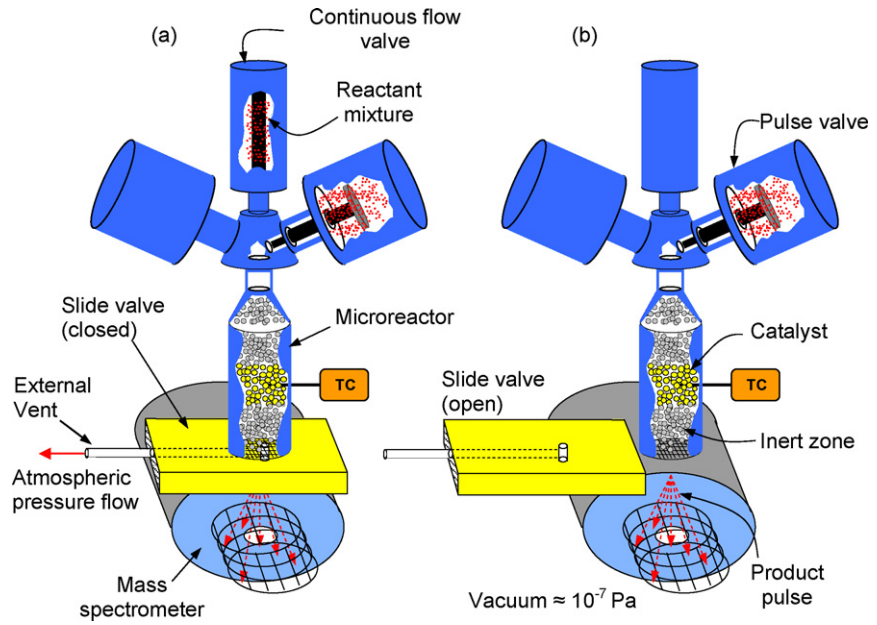

Fig. 22. Illustration of high-pressure (a), and vacuum (b) configurations of TAP reactor system. The microreactor can be shifted from high-pressure operation to vacuum in minutes by opening the slide valve.

introduced through the continuous valve, giving a gas residence time in the reactor of 1.8 s.

The temperature dependence of CO_2 production was obtained by heating or cooling the reactor at a constant rate while maintaining an input flow of 50 cc/min. The internal reactor temperature was ramped from 40 to 430 °C over a 40 min interval. Upon reaching 430 °C, the reactor temperature was held constant for 5 min and then decreased at the same ramp rate to room temperature. A small amount of the reactor effluent was diverted into the mass spectrometer chamber, and its mass spectrum was continuously monitored.

Both TAP vacuum and atmospheric flow data exhibit a turning point in CO_2 production indicating a transition from reaction controlled by one adsorbed species to one controlled by a different

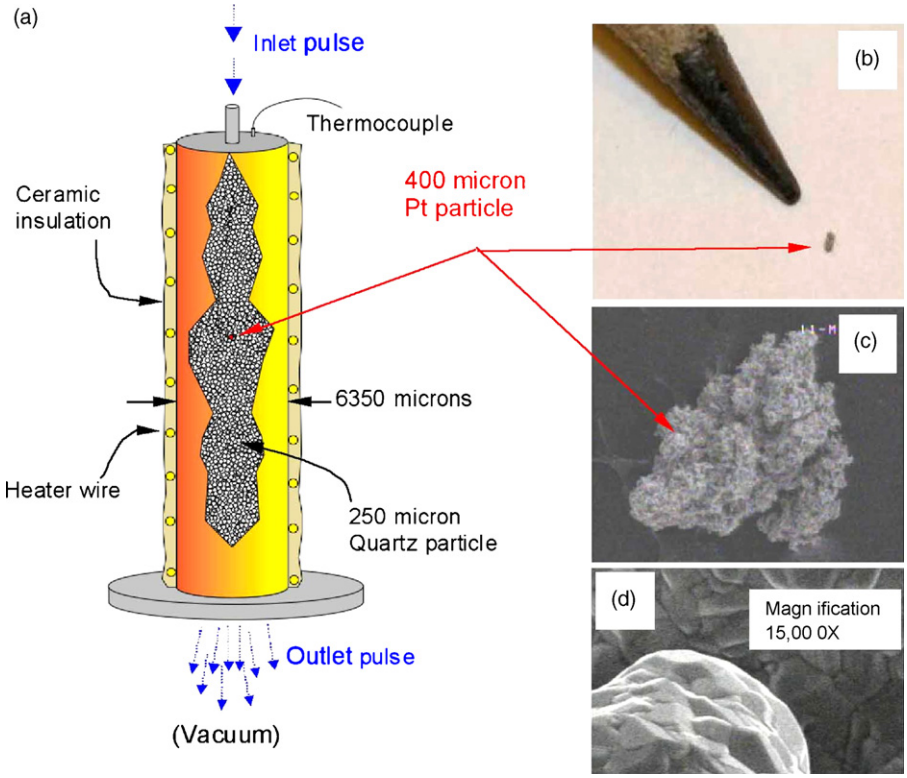

Fig. 23. (a) Schematic of TAP single particle microreactor configuration. The 400 μm diameter Pt particle is packed within a sea of inert quartz particles with diameters between 210 and 250 μm. (b) Image comparing a 400 μm Pt particle to a pencil point. (c) SEM image showing the complex surface structure of a polycrystalline Pt particle. (d) Higher magnification (15,000×) of the particle shown in (c), which shows the surface is non-porous [17].

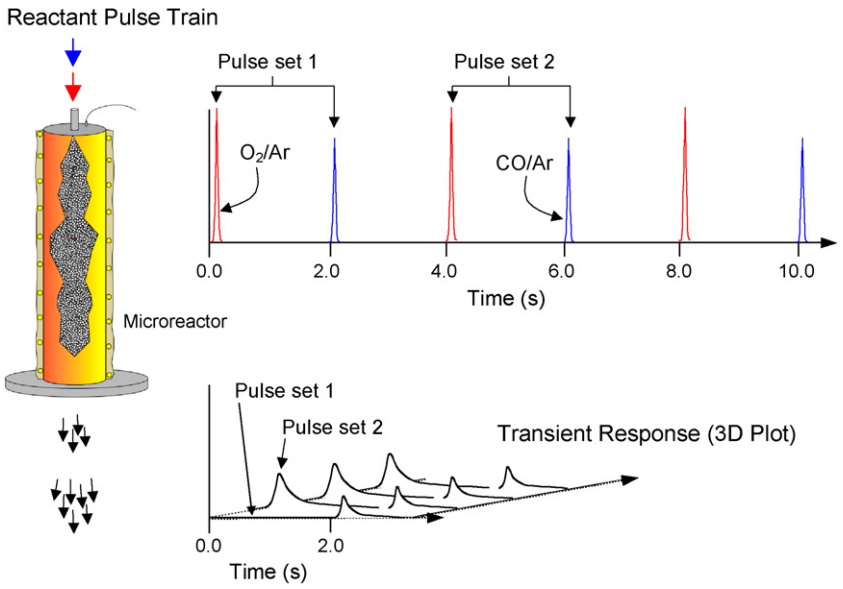

Fig. 24. Illustration of a TAP pump-probe experiment in which O_2/Ar and CO_2/Ar are pulsed in an alternating sequence and the CO_2 transient response is measured during each pulse.

adsorbed species at 170 °C. The upper branch in the CO_2 curve of the atmospheric flow experiment corresponds to an O_2 covered surface, and the lower branch corresponds to a CO covered Pt surface (Fig. 25(b)). From the pulse response data, in the region of the CO_2 maximum, the areas under the CO_2 response curves (CO_2 yield) corresponding to the O_2 and CO pulses are approximately the same, indicating nearly equal coverages of O_2 and CO (Fig. 25(c)). The correspondence in "turning points" indicates that the coverage in vacuum and atmospheric pressure experiments is approximately the same and the intrinsic kinetic data obtained in vacuum experiments can be used to describe kinetic behavior in the atmospheric pressure domain.

Taking the conversion of CO or the CO_2 yield at the "turning point" from vacuum pulse response and atmospheric flow data, the apparent kinetic rate constant can be calculated. In combination with the gas residence time (τ) in the catalyst zone, the apparent kinetic rate constant is given by the following expression:

$$k_{apparent} = \frac{X}{(1-X)\tau}. \tag{40}$$

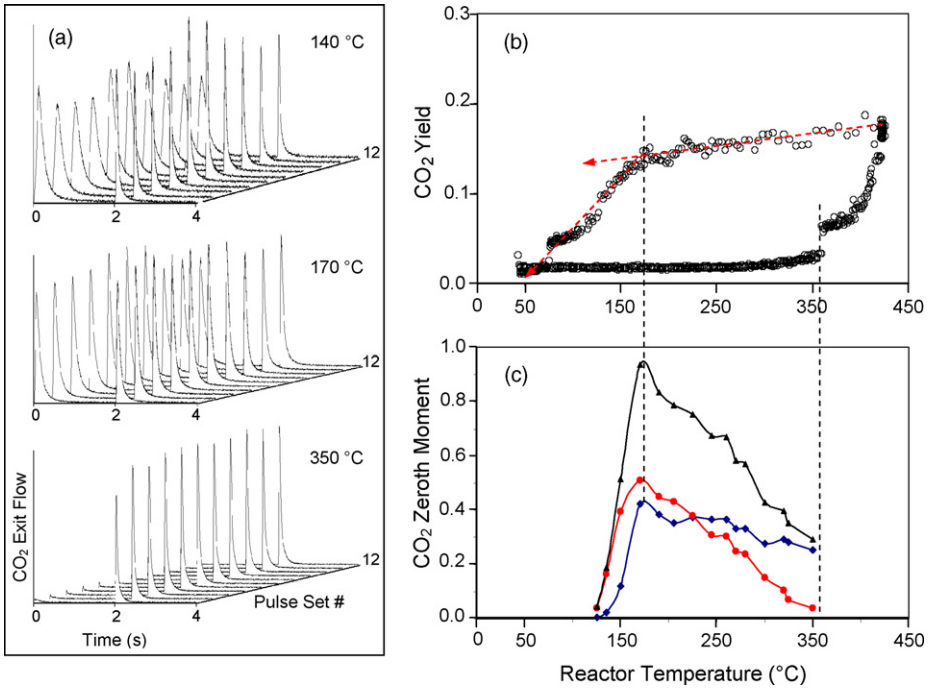

Fig. 25. Comparison of CO_2 produced during TAP vacuum pump-probe experiments and atmospheric flow experiments for CO oxidation over single Pt particle with the same composition of reactants. (a) A typical set of pump-probe CO_2 responses ($m/e = 44$) for reaction at 140, 170, and 350 °C. There is a shift in the amount of CO_2 produced during both CO and oxygen pulses as temperature increases. (b) CO_2 production observed from atmospheric flow experiment. The CO_2 produced while increasing reactor temperature is less than the CO_2 produced during reactor temperature decrease as shown by the counter-clockwise hysteresis loop. (c) CO_2 production observed from vacuum pump-probe experiment. The black line represents the total CO_2 yield. The red and blue lines represent the CO_2 yield on the oxygen pulse and CO pulse, respectively. (For interpretation of the references to color in this figure legend, the reader is referred to the web version of the article.)

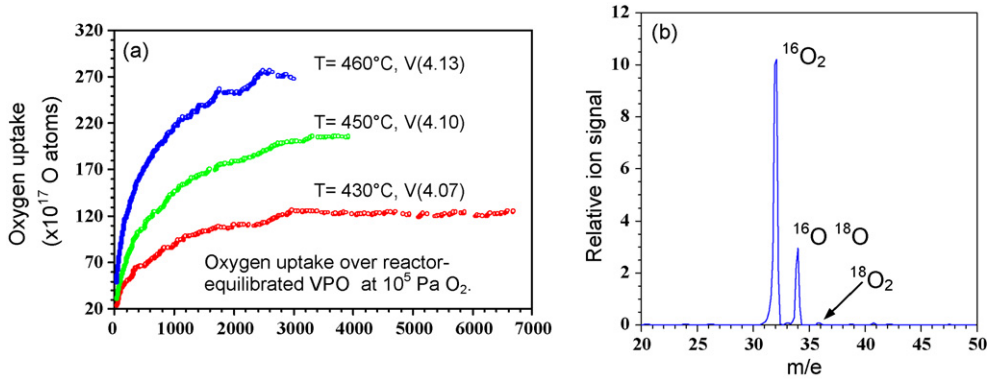

Fig. 26. (a) Oxygen uptake over reactor-equilibrated VPO at 10^5 Pa O_2 and (b) O_2 desorption spectrum under vacuum from $^{18}O_2$-treated $(VO)_2P_2O_7$.

Using an approximate conversion of 90% in the vacuum pulse-response experiment, the apparent kinetic rate constant is calculated to be 9000 s^{-1}. In the atmospheric flow experiment, using a conversion of 20% the apparent kinetic rate constant is calculated to be 9280 s^{-1}. The two apparent constants differ by approximately 3%. Although there may be some error involved in experimentation, the values of the apparent kinetic rate constants are approximately the same. The ability to relate data both qualitatively and quantitatively in the atmospheric pressure domain to the data obtained in vacuum pulse-response experiments using a single Pt particle is a step toward bridging across the pressure gap.

6.2. Tracking the evolution of catalytic properties

Structure–activity correlations can be established using a surface science strategy and measuring reactions on a well-defined model surface. Another approach is based on the application of in situ spectroscopic techniques, which try to measure surface adspecies or identify surface structures that change during reaction. Surface spectroscopy techniques can also be used to characterize catalyst samples before and after reaction. In this case a change in catalyst performance can often be associated with a change in surface composition of structure. Transient kinetic experiments can also be used to indirectly measure changes in the composition and structure while simultaneously measuring changes in kinetic properties. This latter approach is the one adopted in TAP reactor studies, and is illustrated by the following examples.

6.2.1. C_4 oxidation over VPO catalysts

Catalysts based on vanadium oxides are used extensively in selective oxidation processes [56–60,150–153]. The selective oxidation of *n*-butane and other C_4 molecules over vanadyl pyrophosphate (VPO)-based catalysts to maleic anhydride and intermediate compounds (e.g., furan, butadiene and butene) is strongly influenced by the feed conditions, especially the oxygen to hydrocarbon ratio. A combination of atmospheric pressure and TAP pulse-response experiments determined that "reactor-equilibrated" VPO adsorbs oxygen at elevated oxygen pressures to form a more active-selective catalyst [56–60]. If the oxygen-treated catalyst is heated in vacuum the adsorbed oxygen desorbs leaving a less active-selective catalyst. Fig. 26 shows three oxygen uptake curves at 430, 450 and 460 °C and an oxygen pressure of 10^5 Pa, and the oxygen desorption spectrum when an oxygen-18 treated VPO sample is heated in vacuum. The O^{16} to O^{18} ratio indicates that oxygen is only taken up in the first few monolayers of the VPO surface.

Oxygen-treated VPO catalysts were determined to be more active and selective provided the oxidation did not lead to less active $VOPO_4$ phases [56–60]. The oxidation of *n*-butane, and other C_4 compounds was investigated in TAP pulse-response experiments by pulsing a C_4/Ar mixture over VPO and measuring the pulse response curves of the reactants and products. Fig. 27 shows typical response curves and an Arrhenius plot for *n*-butane oxidation over an oxygen-treated catalyst.

The change in kinetic parameters as the surface oxygen concentration is altered is shown in Fig. 28, which plots the activation energy and apparent equilibrium constant for different products at different stages in the reduction of VPO. The mechanistic impli-

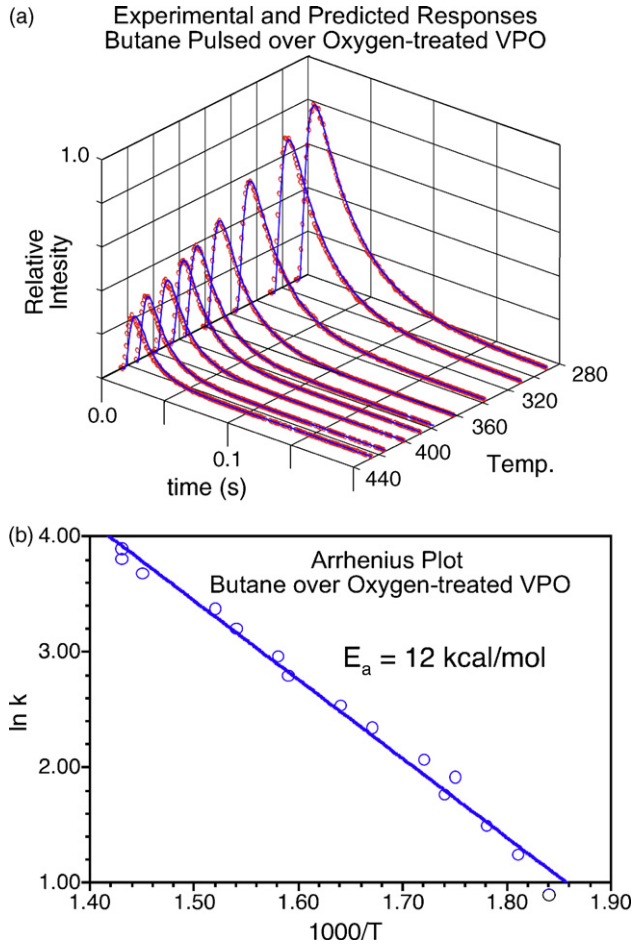

Fig. 27. (a) *n*-Butane pulse response curves over oxygen-treated VPO at various temperatures. Each curve is obtained for the same initial VPO oxidation state. (b) Arrhenius plot obtained from the temperature dependence of the *n*-butane conversion giving an activation energy of 12 kcal/mol.

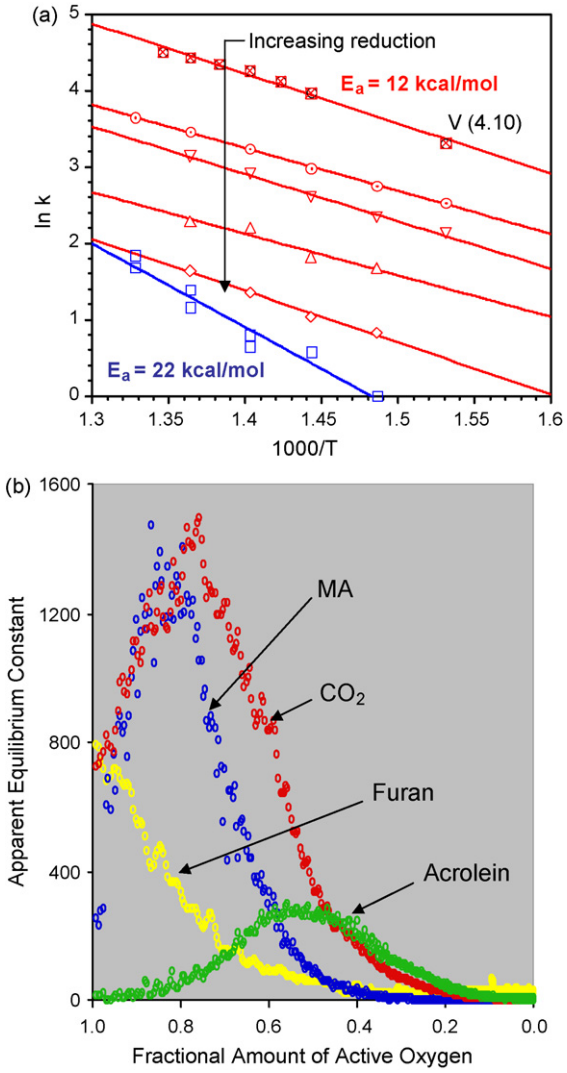

Fig. 28. (a) Arrhenius plots for *n*-butane oxidation over a single VPO sample reduced by a long series of *n*-butane pulses. As the surface is reduced the activation energy increases and (b) apparent equilibrium constant for various products as a function of VPO oxidation state.

cations of the data presented in Figs. 27 and 28 are presented in Section 7.1.3.

6.2.2. Reactive formation of metal deposits

Atomic deposition under ultrahigh vacuum conditions offers a precise method of delivering metal atoms to a solid surface. Fig. 29 shows an atomic beam deposition (ABD) apparatus coupled to a TAP reactor system. The ABD system produces metal atoms by focusing light from a pulsed excimer laser onto the surface of a metal (palladium) target. The energy from the pulse ejects a spray of atoms. Directly beneath the target is a cylindrical sample holder, which has a magnetic diaphragm for vibrating a bed of support particles. Sending a pulsed current through an electromagnetic coil causes the diaphragm to vibrate, continuously agitating the particles to produce a uniform coating of metal atoms. After deposition, samples are transferred to a TAP-2 reactor and kinetically characterized.

In our experiments, we deposited different loadings of Pd atoms onto 210–250 μm diameter inert quartz (SiO_2) particles. The particles were then reduced with a long series of CO pulses while heating the sample in a linear ramp.

CO_2 production resulting from the oxidation of CO/reduction of Pd displayed an interesting oscillatory behavior. The resulting TPR spectrum is shown in Fig. 30 for a sample prepared by exposing the Pd target to 750 Pd laser pulses.

A maximum in CO_2 production is observed at 154 °C. After the maximum, CO_2 production drops rapidly as the sample continues to heat. The initial steep drop in CO_2 production is followed by a gradual decrease with periodic bursts giving the appearance of a damped oscillation. All freshly deposited samples exhibited this oscillatory behavior. The trend in CO_2 production and the total amount produced was highly reproducible on separate samples prepared with identical Pd loadings. Reoxidation of sample followed by reduction did not yield oscillations.

Heuristically, every peak in the dependence in Fig. 30 can be viewed as a typical TPR peak related to a specific form of catalyst oxygen. CO_2 production during the first peak corresponds to the depletion of accessible surface oxygen. Then, the series of peaks that follow can be considered as resulting from reaction of CO with other forms of catalyst oxygen. Thus, abrupt changes in the amount of oxygen indicate abrupt changes in the Pd/PdO composition. The observed phenomenon can be interpreted as an example of reactive self-assembly, the combination of reaction kinetics, diffusion, and surface phase transitions [94,149].

6.3. Surface lifetimes of reactive species

The surface lifetime of an adspecies under reaction conditions is a function of the rate of reaction, the rate of desorption, and the rate at which the adspecies diffuses into the catalyst bulk. The adsorption–desorption characteristics of a species can be determined in TAP pulse-response experiments by comparing the exit-flow curve of the species with the standard diffusion curve (STD) (see Sections 5.2.2 and 5.2.3). If the curve falls inside the STD then the species is irreversibly adsorbed. The surface concentration of an active species can also decrease if the species diffuses into the catalyst bulk or is depleted by reaction with some other surface species. The reactive lifetime of an adspecies can be measured in TAP pump-probe experiments by changing the pump-probe interval.

The reactive lifetime of oxygen on a Pt particle was measured in a series of pump-probe experiments using two separate reactant mixtures of O_2/Ar (70/30 ratio) and CO/Ar (70/30 ratio), which were injected from two separate pulse valves. The mixtures were pulsed in an alternating sequence into a microreactor containing a single 400 μm Pt particle packed in a bed of inert quartz particles. The interval separating the oxygen pulses and the CO pulses was varied between 1 and 9 s. In all cases the pump-probe cycle time was 10 s. Thus when the interval between the oxygen and CO pulse is 5 s, the interval between the CO and following oxygen pulse is also 5 s. Fig. 31 shows the CO_2 production for different pump-probe intervals at 150 and 350 °C.

CO_2 production on the oxygen pulse at 350 °C is significantly lower than production at 150 °C. It is independent of the pump-probe interval. CO_2 production on the CO pulse at 150 °C is also independent of the pump-probe interval. At 350 °C, CO_2 decreases with the pump-probe interval. The drop in CO_2 production can be attributed to a decrease in the amount of active oxygen. The rate of the drop in active oxygen can be calculated from the zeroth moments of the CO_2 and is plotted in Fig. 32.

7. Unraveling complex catalytic mechanisms using TAP pulse-response experiments

7.1. Qualitative information on mechanisms

TAP transient response data provides the identity, amount, and time dependence of the flow of different species exiting the TAP microreactor. The response data is a sensitive function of the trans-

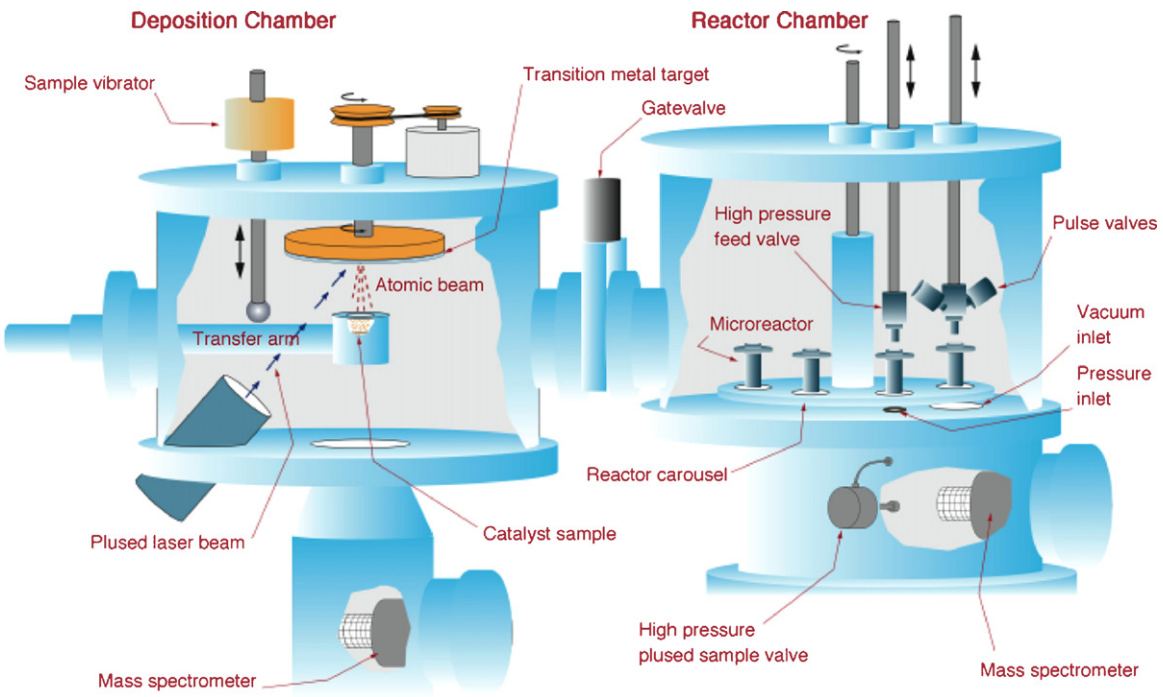

Fig. 29. Schematic of atomic beam deposition system coupled to a TAP-2 reactor system [94].

port process, the temperature, and gas–solid interactions. It is standard practice to use an inert gas (typically argon) as an internal reference. At reaction temperatures, the total time inert gas molecules spend interacting with the solid is negligible, and the inert gas response can be assumed to be solely a function of the gas transport process and temperature. Under Knudsen flow conditions an inert gas response is described by the "standard diffusion curve" (see Section 5.2.1). The standard diffusion curve for any gas with a unique molecular weight at any temperature can be constructed from the inert gas response. Deviation from the standard diffusion curve is evidence of a gas–solid interaction.

Catalytic reaction mechanisms represent the sequence of molecular level processes that occur during a single catalytic cycle. Processes typically included in a mechanism are reactant adsorption and desorption, surface diffusion, surface reaction, and product desorption and re-adsorption. The mechanism may also include structural and compositional changes that occur in the catalyst. Experimental data on such changes are very useful for developing structure–activity relationships. Constructing a detailed mechanism requires knowledge of the different species (reactants, surface complexes, catalyst components, desorbing intermediates, and products) participating in the overall reaction, and the time

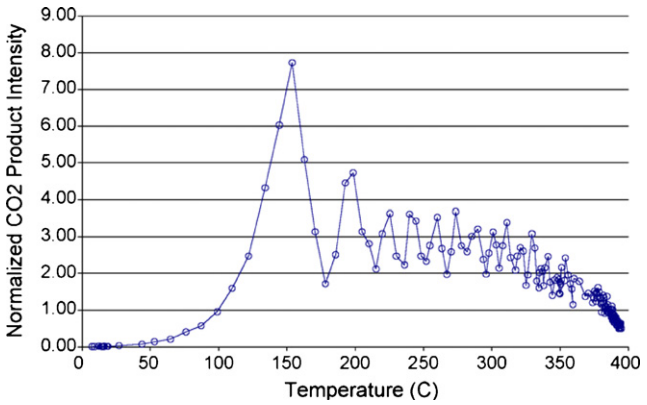

Fig. 30. Normalized CO_2 production (determined by measuring the zeroth moment of the CO_2 responses) over fresh Pd deposits (750 pulses) obtained by pulsing CO and ramping the reactor temperature from 32 to 400 °C [94].

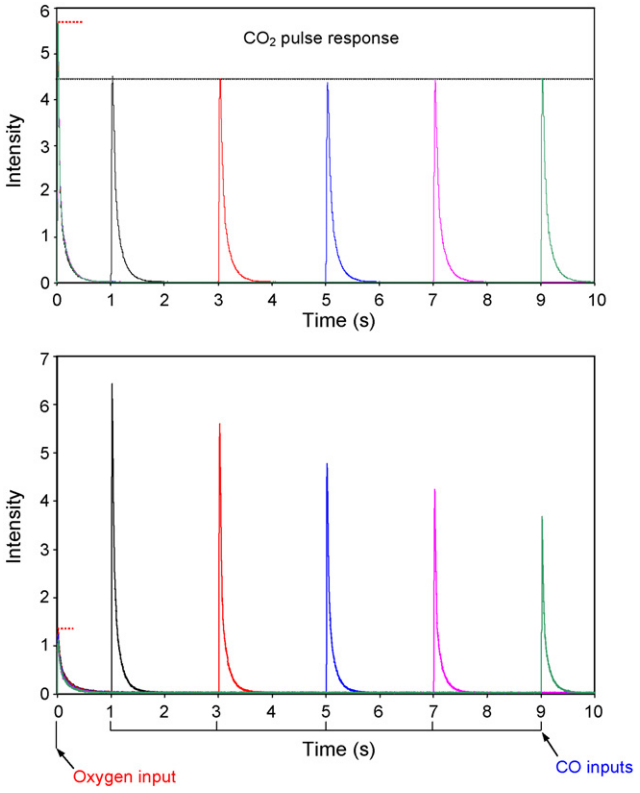

Fig. 31. Pump-probe data showing CO_2 production as a function of temperature and pump-probe interval. At 150 °C the CO_2 production is essentially independent of the pump-probe interval out to 9 s separation. At 350 °C the CO_2 production drops as the pump-probe interval increases indicating a drop in the active oxygen concentration with time.

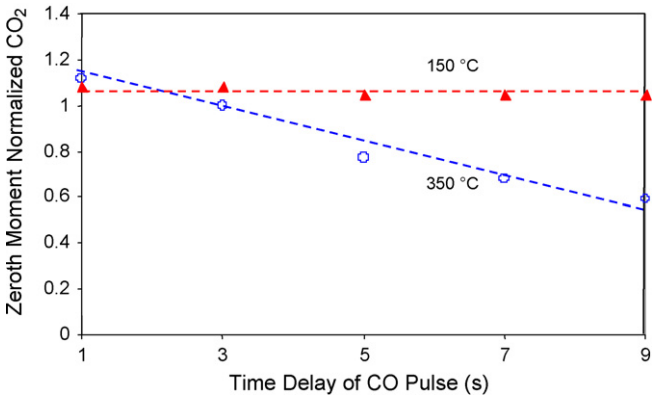

Fig. 32. Normalized CO_2 production on the CO pulse calculated from the zeroth moment of the pulse response curve. CO_2 production is constant at 150 °C, and drops to ≈0.5 times its value in 9 s at 350 °C.

of their appearance in the sequence of steps. TAP experiments provide direct information on reactants, products, and desorbing intermediates, and indirect information on surface complexes and catalyst components. Different types of TAP experiments provide unique information on the sequence of steps in the overall reaction, on the lifetime of surface adspecies, the diffusion of catalyst components, the influence of different surface concentrations on the rate and energetics of various surface processes.

The types and sequence of TAP experiments performed during a catalytic study are often motivated by questions that naturally arise during the construction of a reaction mechanism. Interaction between the experiment and the researcher can be viewed as "conversational", *i.e.*, an experiment, based on a simple question provides data, that raises a new question, which in turn suggests a new experiment, and so on. The sequence of questions and answers can follow one another rapidly because a single TAP pulse response typically takes only a few seconds.

7.1.1. Single pulse information

Initial data on the adsorption/desorption of pure gases (reactants, products and intermediates) over catalytic and inert materials can be obtained by comparing the shape of their pulse response curves to a standard diffusion curve. Simple qualitative analysis based on well-defined theoretical patterns [14,32] (see Sections 5.2.2 and 5.2.3) can be used to compare the adsorption strength of different molecules, to determine if an adsorption process is reversible or irreversible, and to determine if molecules compete for the same adsorption sites. Changes in the pulse shape of a single species over a series of pulses can reveal how the surface properties of a catalyst change during reaction. For example, pulsing CO or a hydrocarbon over a mixed-metal oxide or metal catalyst pretreated by oxygen will reveal how adsorption properties change as the surface oxygen is depleted.

Qualitative comparison of reactant and product pulse shapes can be used to construct a multistep reaction sequence. For example, in TAP-1 studies using a three-zone reactor, the reaction of methanol over an H-ZSM-5 zeolite [32,160] produced olefins (especially propylene), water, dimethyl ether, formaldehyde and methane. Compared to the standard diffusion curve, the methanol and product responses were all very broad. From shifts in the pulse maxima, the pulse widths, and pulse decay curves the methanol adsorption process and product formation sequence was deduced. The shape of the methanol pulse indicates it spends a significant amount of time on the catalyst, but is reversibly adsorbed. The water response is similar to the methanol response indicating a rapid exchange process and that water adsorption is similar to methanol. Based on the relative shapes of the remaining product response curves the following reaction mechanism was proposed [32,160]. Methanol dehydrates to dimethyl ether, which reacts further to olefins. The production of dimethyl ether proceeds via the dissociative adsorption of methanol which forms water and a methoxy group. The methoxy group reacts with methanol to produce adsorbed dimethyl ether. Propylene and ethylene are formed from dimethyl ether and involve a common surface intermediate, which can decompose to form ethylene or react with adsorbed methanol to give propylene and water. Higher olefins are produced via reaction of lighter olefins with methoxy groups on the surface.

7.1.2. Pump-probe information

TAP pump-probe experiments provide a means of adding reactants to the surface of a catalyst in sequence, and precisely controlling the time interval between reactant inputs. Typically, the gas-phase component of one reactant is no longer present in the reactor when the other reactant is introduced. Pump-probe experiments can be used to study processes that involve rapid changes in the concentration of a reactive adspecies. The use of isotopes can help distinguish between mechanistic routes that produce the same product. The pump-probe format can also be used to distinguish processes that involve bulk diffusion from surface processes, and can provide information on the reactive formation of catalytic sites. Pump-probe experiments were used to study the activation of silver powder, and subsequent epoxidation of ethylene [95], in a TAP-1 reactor using a one-zone reactor. Experiments involved injecting an alternating sequence of oxygen and ethylene-d_4 pulses into the microreactor using a fixed pump-probe interval and monitoring the CO_2 and ethylene oxide yield as a function of the O_2/C_2D_4 ratio. Experiments were also performed using fixed amounts of reactants at different pump-probe time intervals and monitoring C_2D_4O as a function of the pump-probe interval. In experiments using a fixed pump-probe interval, ethylene oxide production was observed during the ethylene pulse, but not during the oxygen pulse. CO_2 production occurred during both pulses. The amount of both products increased nearly linearly with the size of the oxygen pulse for a O_2/C_2D_4 ratio below 0.6 and was nearly independent of the O_2 pulse size for high O_2/C_2D_4 ratios. The results indicate that the rate of ethylene oxidation depends on the concentration of adsorbed oxygen and that selective oxidation to ethylene oxide involves the reaction of ethylene with adsorbed oxygen species. Comparison of the ethylene and ethylene oxide pulse shapes indicate no measurable reaction time, as both species appear simultaneously at the reactor exit. The surface lifetime of active oxygen species was investigated by measuring the C_2D_4O product yield as a function of the pump-probe interval. The maximum C_2D_4O yield occurred at a large time interval, when gas-phase oxygen is close to zero, and the amount of adsorbed oxygen is at a maximum. The results were interpreted to mean that the formation of the active oxygen species involves a slow step in which atomically adsorbed oxygen becomes associated with a partially oxidized silver cluster, and that the active oxygen has a long surface lifetime. The experiments provided clear evidence that the active oxygen species are atomically adsorbed oxygen species, and not molecularly adsorbed oxygen.

Experiments involving the oxidation of CO over a Pt catalyst (see Section 6.3), using different pump-probe intervals indicate that the active surface oxygen is rapidly depleted at higher reaction temperatures immediately after an oxygen pulse. The disappearance can be attributed to oxygen exchange between the catalyst surface and bulk.

In general, the broadening of the pulse response of a product in comparison to a reactant is evidence of one or more surface intermediates participating in a complex surface reaction. The dependence of the exit flow on the pump-probe interval indicates a parallel process that depletes one of the surface reactants.

7.1.3. Multi-pulse TAP experiments

TAP experiments usually involve a series of single or alternating pulses containing fixed concentrations of reactants and inert reference gas. A single reactant can be used to produce a controlled change in the catalyst surface composition. For example, CO, hydrogen, or a hydrocarbon can be pulsed over a mixed-metal oxide to deplete the surface oxygen, and change the oxidation state of surface metal ions. At the same time the transient responses of reactants and products over the course of the reduction can be used to monitor changes in reaction products and in catalytic properties. Reduction of a mixed-metal oxide strongly influences its adsorption properties, and can cause a change in the reaction mechanism. Comparison of changes in catalytic properties with changes in surface composition provides information to develop activity–structure or activity–composition relationships, and to construct models of the active catalytic site.

TAP multipulse experiments using a TAP-2 reactor system with three-zone and thin-zone microreactor configurations were used to investigate the dependence of kinetic parameters for hydrocarbon oxidation on VPO catalysts as a function of the oxygen surface concentration [170,171]. Typical experimental results are shown in Figs. 27 and 28 in Section 6.2.1. Catalysts were initially heated in an oxygen atmosphere, and the oxygen uptake was measured as a function of temperature and O_2 partial pressure. Oxygen was readily adsorbed at temperatures above 400 °C, in amounts totaling 1–3 monolayers (see Fig. 26). The resulting "oxygen-treated" catalyst was then reduced with a hydrocarbon (e.g., *n*-butane, butene, butadiene and furan) in series of anaerobic pulses at different temperatures (see Fig. 27a). Arrhenius plots obtained from the pulse response data for different VPO oxidation states is plotted in Figs. 27b and 28a. The data shows that the number of active sites or active oxygen species decreases as the catalyst is reduced and the activation energy for *n*-butane conversion increases. The conversion increases suddenly without a significant decrease in the surface oxygen concentration indicating the reaction shifts to a different active site (active oxygen species). The rapid change can be explained as follows: energy of activation changes linearly with the change in surface composition and therefore, the kinetic constant and conversion change exponentially with the composition as well. Similar experiments were performed with other hydrocarbons, and it was found that both the product spectrum and kinetic parameters (Fig. 28b) were a strong function of the hydrocarbon reactant and the VPO oxidation state. During butane oxidation experiments it was found that reaction intermediates such as butene, butadiene, and furan formed and desorbed at lower surface oxygen concentrations, their production at higher surface oxygen concentrations was suppressed.

7.2. Quantitative information on mechanisms

Models that describe the transport-kinetic processes that typically occur in TAP pulse-response experiments are parabolic partial differential equations (see Section 5). Typically, the model parameters are extracted from the pulse response data by using parameter estimation methods. A review of different methods for parameter estimation from TAP pulse response data was recently presented by Schuurman [162]. Different approaches based on analytical solutions have been developed during the last decade and include the moment-based approach [32–34] and the global-transfer matrix approach [118,119,123,124].

The moment-based approach is well established and compares the analytical expressions for the zeroth, first and second moments of the model-based pulse response to the moments that are evaluated from the TAP response data. Parameters such as the effective diffusivity and kinetic constants can be obtained. Different mechanisms and corresponding models can be compared and discriminated using these expressions. In the case of the global-transfer matrix approach, the general theory of the pulse-response–pulse experiment for the multi-zone configuration has been described. The theory offers an efficient means to compute the actual profiles of gas and surface concentration in the reactor as well as the corresponding values at the reactor exit using the fast Fourier transform. For the thin-zone TAP reactor (TZTR) in which the gas and catalyst composition are nearly uniform, the theoretical expressions are very simplified (see Section 5.4 [109,112]). In this case, every substance can be characterized by three apparent parameters obtained using three observed moments, *i.e.*, the apparent kinetic constant, the time delay, and 'equilibrium constant' [33,163]. These expressions have been used for developing a new strategy for kinetic characterization of states in a TAP reactor with multi-pulse responses that is called "state-by-state-kinetic screening". This strategy was illustrated using furan oxidation over a VPO catalyst [33]. Essential information on the apparent parameters as a function of the catalyst oxidation/reduction degree and comparative analysis of these parameters create a basis for developing a detailed reaction mechanism. For example, calculations demonstrate that apparent kinetic constants for all products (maleic anhydride, acrolein, and CO_2) are clearly different at all oxidation/reduction degrees. Thus, the reaction routes for all products should be distinguishable. The non-linear dependence of apparent kinetic constants on the oxidation degree is explained by assuming a reaction with participation of catalyst oxygen, particularly subsurface oxygen. Time delays for all mentioned products are clearly distinguished as well, and the number of distinguished time delays indicates the number of surface intermediates. The proposed mechanism must include at least three independent routes involving at least four surface intermediates.

Recently, a new procedure, the so-called Y-procedure [148], was developed for determining the gas concentration and reaction rate in the active zone of the thin-zone TAP reactor (TZTR) without making any assumptions on the detailed mechanism and corresponding kinetic dependence. Hence, the method is essentially independent of the kinetic model. The mathematical basis of this procedure is a Laplace-domain analysis of two inert zones in a TZTR followed by transposition to the Fourier-transform domain. When combined with time discretization and filtering, the Y-procedure leads to an efficient and practical method for reconstructing the kinetic dependences in the catalyst zone. It also can be considered as a basis for advanced software for non-steady-state kinetic data interpretation and detail mechanism development.

In summary, a variety of mathematical techniques have been developed for parameter estimation from theoretical models of the transport-kinetics interactions that occur in the TAP reactor using pulse response data. Some of these are traditional methods that have a well-established history in the transient response literature for catalytic systems. Newer tools that recognize the unique operating features of the TAP reactor, such as the "Y-procedure", have also been developed and provide a simple yet robust approach for extracting fundamental kinetic and other surface-related parameters. It is expected that the increased development of new software tools for solution of partial differential equations as well as user interfaces will lead to a new generation of methods that allow robust analysis to be performed using a large range of TAP pulse response data sets.

8. Summary

The TAP reactor system provides the catalyst scientist with a unique capability to unravel the chemistry, kinetics, and mechanisms of gas–solid catalyzed reactions using a variety of transient response protocols. These protocols and the associated knowledge have been developed over a period of 20+ years, and are based

upon several hundred man-years of research effort. The development of various commercial versions of the TAP reactor system has allowed a wide cross-section of both academic and industrial research groups to use the technology on a variety of challenging applications. These collective efforts have created new fundamental and practical knowledge on complex industrial catalysts for a variety of important chemistries, some of which have been highlighted in the paper. In closing, it is useful to mention some research thrusts in TAP technology that will allow a broader cross-section of catalyst scientists to address emerging challenges in catalytic science and technology, such as those associated with clean energy systems and the environment. In terms of advanced analytical capabilities, coupling of the TAP system to a broader range of mass spectroscopy and spectroscopic instrumentation will provide simultaneous collection of real-time transient and steady-state response data on both gas-phase and surface species. Coupling of the TAP system to an angular reflectron time-of-flight mass spectrometer has been demonstrated. The concept of a *Coupled Array* is also under development and will allow the TAP system to serve as a type of catalyst analytical "engine" that can be directly coupled to other systems that either generate catalyst particles with unique properties, or which provide advanced tools for catalyst characterization. Coupling will be accomplished using special-purpose particle transport systems and robotic units that will allow small aliquots of catalyst particles (on the order of tens of milligrams) to be transferred back and forth between user-selected array elements and the TAP system engine. Examples of these array elements might include catalyst surface modification systems, catalyst synthesis workstations, catalyst activity testing systems, catalyst libraries, and even lab or pilot-scale reactors involving moving solids, such as hot fluidized beds. A special-purpose automation and control system will allow catalyst scientists located at a remote location to define and conduct TAP experiments using one of several strategically located *Coupled Array* systems. A suite of data modeling tools will allow fundamental kinetic and other related parameters to be extracted from the data. This approach will permit them to focus on experimental aspects, and also enhance interactions between other catalyst scientists in a type of cyber-enabled discovery and innovation platform for catalytic systems.

References

[1] I.E. Maxwell, P. van den Brink, R.S. Downing, A.H. Sijpkes, S. Gomez, Th. Maschmeyer, Top. Catal. 24 (2003) 125–135.
[2] R.A. Potyrailo, E.J. Amis, High Throughput Analysis: A Tool for Combinatorial Materials Science, Kluwer Academic Publishers, New York, 2003.
[3] Y.L. Dar, Macromol. Rapid Commun. 25 (2004) 34–47.
[4] M.A.R. Meier, U.S. Schubert, J. Mater. Chem. 14 (2004) 3289–3299.
[5] D.W. Goodman, Chem. Rev. 95 (1995) 523–536.
[6] C.R. Henry, Surf. Sci. Rep. 31 (1998) 231–325.
[7] G.A. Somorjai, B.E. Bent, Phys. Today 48 (1995) 58.
[8] G.A. Somorjai, Chem. Rev. 96 (1996) 1223–1235.
[9] H.P. Bonzel, Surf. Sci. 68 (1977) 236.
[10] C.T. Campbell, Surf. Sci. Rep. 27 (1997) 1–111.
[11] H. Happel, Isotopic Assessment of Heterogeneous Catalysis, Academic Press, Orlando, 1986.
[12] P.L. Silveston, Composition Modulation of Catalytic Reactors, Gordon and Breach, Ontario, 1998.
[13] C.O. Bennett, Adv. Catal. 44 (2000) 329–416.
[14] J.T. Gleaves, G.S. Yablonskii, P. Phanawadee, Y. Schuurman, Appl. Catal. A: Gen. 160 (1997) 55–88.
[15] J. Pérez-Ramírez, E.V. Kondratenko (Eds.), Catal. Today 121 (2007) 1–124.
[16] J.T. Gleaves, J.R. Ebner, T.C. Kuechler, Catal. Rev. -Sci. Eng. 30 (1988) 49–116.
[17] X. Zheng, J.T. Gleaves, G.S. Yablonsky, T. Brownscombe, A. Gaffney, M. Clark, S. Han, Appl. Catal. A: Gen. 341 (2008) 86–92.
[18] R. Feres, G.S. Yablonsky, A. Mueller, A. Baerstein, X. Zheng, J.T. Gleaves, Chem. Eng. Sci. 64 (2009) 568–581.
[19] J.T. Gleaves, J.R. Ebner, U.S. Patent 4,626,412 assigned to Monsanto Company, December 2, 1986.
[20] J.T. Gleaves, J.R. Ebner, P.L. Mills, Studies in Surface Science and Catalysis, vol. 38, Elsevier, Amsterdam, 1988.
[21] J. Libuda, H.-J. Freund, Surf. Sci. Rep. 57 (2005) 157–298.
[22] M. Valden, J. Aaltonen, E. Kuusisto, M. Pessa, C.J. Barnes, Surf. Sci. 307–309 (1994) 193–198.
[23] M.P. D'Evelyn, R.J. Madix, Surf. Sci. Rep. 3 (1984) 413.
[24] J.A. Barker, D.J. Auerbach, Surf. Sci. Rep. 4 (1985) 1.
[25] M. Asscher, G.A. Somorjai, G. Scoles (Eds.), Atomic and Molecular Beam Methods, vol. 2, Oxford University Press, 1988.
[26] M.L. Yu, L.A. Delouise, Surf. Sci. Rep. 19 (1994) 285.
[27] C.T. Rettner, D.J. Auerbach, J.C. Tully, A.W. Kleyn, J. Phys. Chem. 100 (1996) 13021.
[28] A.W. Kleyn, Chem. Soc. Rev. 32 (2003) 87.
[29] A.W. Kleyn, D.P. Woodruff (Eds.), The Chemical Physics of Solid Surfaces (Surface Dynamics), vol. 11, Elsevier, Amsterdam, 2003.
[30] J. Libuda, H.-J. Freund, J. Phys. Chem. B 106 (2002) 4901.
[31] J. Libuda, Chem. Phys. Chem. 5 (2004) 625.
[32] G.S. Yablonsky, M. Olea, G.B. Marin, J. Catal. 216 (2003) 120–134.
[33] S.O. Shekhtman, G.S. Yablonsky, J.T. Gleaves, R. Fushimi, Chem. Eng. Sci. 58 (2003) 4843–4859.
[34] G.S. Yablonskii, S.O. Shekhtman, S. Chen, J.T. Gleaves, Ind. Eng. Chem. Res. 37 (1998) 2193–2202.
[35] D.Z. Wang, O. Dewaele, G.F. Froment, J. Mol. Catal. A: Chem. 136 (1998) 301.
[36] O.P. Keipert, M. Baerns, Chem. Eng. Sci. 53 (1998) 3623.
[37] O. Dewaele, D.Z. Wang, G.F. Froment, J. Mol. Catal. A: Chem. 149 (1999) 263.
[38] O. Dewaele, G.F. Froment, Appl. Catal. A 185 (1999) 203.
[39] T.A. Nijhuis, L.J.P. Van Den Broeke, M.J.G. Linders, M. Makkee, F. Kapteijn, J.A. Moulijn, Catal. Today 53 (1999) 189.
[40] A.H.J. Colaris, J. Hoebink, M. de Croon, J.C. Schouten, AIChE J. 48 (2002) 2587.
[41] J.A. Delgado, T.A. Nijhuis, F. Kapteijn, J.A. Moulijn, Chem. Eng. Sci. 59 (2004) 2477.
[42] C. Breitkopf, J. Mol. Catal. A: Chem. 226 (2005) 269.
[43] E.V. Kondratenko, O. Buyevskaya, M. Baerns, J. Mol. Catal. A: Chem. 158 (2000) 199.
[44] B. Silberova, R. Burch, A. Goguet, C. Hardacre, A. Holmen, J. Catal. 219 (2003) 206.
[45] O. Dewaele, G.F. Froment, J. Catal. 184 (1999) 499.
[46] E.V. Kondratenko, O.V. Buyevskaya, M. Soick, M. Baerns, Catal. Lett. 63 (1999) 153.
[47] O.V. Buyevskaya, M. Rothaemel, H.W. Zanthoff, M. Baerns, J. Catal. 146 (1994) 346.
[48] O.V. Buyevskaya, M. Baerns, Catal. Today 21 (1994) 301.
[49] G.A. Martin, C. Mirodatos, Fuel Process. Technol. 42 (1995) 179.
[50] D.J. Statman, J.T. Gleaves, D. McNamara, P.L. Mills, G. Fornasari, J.R.H. Ross, Appl. Catal. 77 (1991) 45.
[51] E.P.J. Malens, J.H.B.L. Hoebink, G.B. Marin, Stud. Surf. Sci. Catal. 81 (1994) 205.
[52] O.V. Buyevskaya, D. Wolf, M. Baerns, Catal. Lett. 29 (1994) 249–260.
[53] O.V. Buyevskaya, K. Walter, D. Wolf, M. Baerns, Catal. Lett. 38 (1996) 81.
[54] M. Soick, O. Buyevskaya, M. Hohenberger, D. Wolf, Catal. Today 32 (1996) 163.
[55] M. Fathi, A. Holmen, F. Monnet, Y. Schuurman, C. Mirodatos, J. Catal. 190 (2000) 439.
[56] U. Rodemerck, B. Kubias, H.W. Zanthoff, M. Baerns, Appl. Catal. A 153 (1997) 203.
[57] U. Rodemerck, B. Kubias, H.W. Zanthoff, G.U. Wolf, M. Baerns, Appl. Catal. A 153 (1997) 217.
[58] J.T. Gleaves, G. Centi, Catal. Today 16 (1993) 69.
[59] B. Kubias, U. Rodemerck, H.W. Zanthoff, M. Meisel, Catal. Today 32 (1996) 243.
[60] P.L. Mills, H.T. Randall, J.S. McCracken, Chem. Eng. Sci. 54 (1999) 3709.
[61] A. Pantazidis, S.A. Bucholz, H.W. Zanthoff, Y. Schuurman, C. Mirodatos, Catal. Today 40 (1998) 207.
[62] O.V. Buyevskaya, M. Baerns, Catal. Today 42 (1998) 315.
[63] Y. Schuurman, T. Decamp, J.C. Jalibert, C. Mirodatos, Stud. Surf. Sci. Catal. 122 (1999) 133.
[64] E.V. Kondratenko, O.V. Buyevskaya, M. Baerns, Top. Catal. 15 (2001) 175.
[65] E.V. Kondratenko, J. Pérez-Ramírez, Appl. Catal. A 267 (2004) 181.
[66] E.V. Kondratenko, M. Cherian, M. Baerns, Catal. Today 99 (2005) 59.
[67] M. Olea, M. Florea, I. Sack, R.P. Silvy, E.M. Gaigneaux, G.B. Marin, P. Grange, J. Catal. 232 (2005) 152.
[68] D.S. Lafyatis, G.F. Froment, A. Pasauclaerbout, E.G. Derouane, J. Catal. 147 (1994) 552.
[69] Y. Schuurman, C. Marquez-Alvarez, V.C.H. Kroll, C. Mirodatos, Catal. Today 46 (1998) 185.
[70] Y. Schuurman, A. Pantazidis, C. Mirodatos, Chem. Eng. Sci. 54 (1999) 3619.
[71] Y. Schuurman, C. Mirodatos, P. Ferreira-Aparicio, I. Rodriguez-Ramos, A. Guerrero-Ruiz, Catal. Lett. 66 (2000) 33.
[72] V. Fierro, Y. Schuurman, C. Mirodatos, J.L. Duplan, J. Verstraete, Chem. Eng. J. 90 (2002) 139.
[73] A.M. O'Connor, Y. Schuurman, J.R.H. Ross, C. Mirodatos, Catal. Today 115 (2006) 191.
[74] V.A. Kondratenko, M. Baerns, J. Catal. 225 (2004) 37.
[75] J. Pérez-Ramírez, E.V. Kondratenko, M.N. Debbagh, J. Catal. 233 (2005) 442.
[76] E.V. Kondratenko, J. Pérez-Ramírez, Appl. Catal. B 64 (2006) 35.
[77] J. Pérez-Ramírez, F. Kapteijn, G. Mul, J.A. Moulijn, J. Catal. 208 (2002) 211.
[78] E.V. Kondratenko, J. Pérez-Ramírez, Catal. Lett. 91 (2003) 211.
[79] K.S. Kabin, P. Khanna, R.L. Muncrief, V. Medhekar, M.P. Harold, Catal. Today 1145 (2006) 72.
[80] C. Rottlander, R. Andorf, C. Plog, B. Krutzsch, M. Baerns, Appl. Catal. B 11 (1996) 49.
[81] T. Gerlach, M. Baerns, Chem. Eng. Sci. 54 (1999) 4379.

[82] E.V. Kondratenko, V.A. Kondratenko, M. Richter, R. Fricke, J. Catal. 239 (2006) 23.
[83] C.S. Heneghan, G.J. Hutchings, S.R. O'Leary, S.H. Taylor, V.J. Boyd, I.D. Hudson, Catal. Today 54 (1999) 3.
[84] M. Bron, E. Kondratenko, A. Trunschke, P. Claus, Z. Phys. Chem. 218 (2004) 405.
[85] J. Pérez-Ramírez, E.V. Kondratenko, V.A. Kondratenko, M. Baerns, J. Catal. 227 (2004) 90.
[86] J. Pérez-Ramírez, E.V. Kondratenko, Chem. Commun. (2004) 376.
[87] J. Pérez-Ramírez, E.V. KOndratenko, V.A. Kondratenko, M. Baerns, J. Catal. 229 (2005) 303.
[88] M. Baerns, R. Imbihl, V.A. Kondratenko, R. Kraehnert, W.K. Offermans, R.A. van Santen, A. Scheibe, J. Catal. 232 (2005) 226.
[89] E.V. Kondratenko, J. Pérez-Ramírez, Appl. Catal. A 289 (2005) 97.
[90] T.A. Nijhuis, M. Makkee, A.D. van Langeveld, J.A. Mouijn, Appl. Catal. A 164 (1997) 237.
[91] M. Olea, M. Kunitake, T. Shido, Y. Iwasawa, Phys. Chem. Chem. Phys. 3 (2001) 627.
[92] S.T. Daniells, A.R. Overweg, M. Makkee, J.A. Moulijn, J. Catal. 230 (2005) 52.
[93] Z.X. Song, H. Nishiguchi, W. Liu, Appl. Catal. A 396 (2006) 175.
[94] R. Fushimi, J.T. Gleaves, G.S. Yablonsky, A. Gaffney, M. Clark, S. Han, Catal. Today 121 (2007) 170–186.
[95] J.T. Gleaves, A.G. Sault, R.J. Madix, J.R. Ebner, J. Catal. 121 (1990) 202.
[96] G.D. Svoboda, J.T. Gleaves, P.L. Mills, Stud. Surf. Sci. Catal. 82 (1994) 481.
[97] G. Creten, F.D. Kopinke, G.F. Froment, Can. J. Chem. Eng. 75 (1997) 882.
[98] G. Creten, D.S. Lafyatis, G.F. Froment, J. Catal. 154 (1995) 151.
[99] D.R. Coulson, P.L. Mills, K. Kourtakis, P. Wijnen, J.J. Lerou, L.E. Manzer, Stud. Surf. Sci. Catal. 75 (1993) 2015.
[100] A. Hinz, B. Nilsson, A. Andersson, Chem. Eng. Sci. 55 (2000) 4385.
[101] A. Setiabudi, J.L. Chen, G. Mul, M. Makkee, J.A. Moulijn, Appl. Catal. B 51 (2004) 9.
[102] A. Bueno-Lopez, K. Krishna, M. Makkee, J.A. Moulijn, J. Catal. 230 (2005) 237.
[103] A. Bueno-Lopez, K. Krishna, M. Makkee, J. Moulijn, Catal. Lett. 99 (2005) 203.
[104] A. Martin, Y. Zhang, H.W. Zanthoff, M. Meisel, M. Baerns, Appl. Catal. A 139 (1996) L11.
[105] F. Konietzni, H.W. Zanthoff, W.F. Maier, J. Catal. 188 (1999) 154.
[106] C. Freitag, S. Besselmann, E. Loffler, W. Grunert, F. Rosowski, M. Muhler, Catal. Today 91–92 (2004) 143.
[107] D.A. Bulushev, E.A. Ivanov, S.I. Reshetnikov, L. Kiwi-Minsker, A. Renken, Chem. Eng. J 107 (2005) 147.
[108] G.S. Yablonsky, S.O. Shekhtman, J.T. Gleaves, P. Phanawadee, Catal. Today 64 (2001) 227.
[109] S.O. Shekhtman, G.S. Yablonsky, S. Chen, J.T. Gleaves, Chem. Eng. Sci. 54 (1999) 4371.
[110] P. Phanawadee, S.O. Shekhtman, C. Jarungmanorom, G.S. Yablonsky, J.T. Gleaves, Chem. Eng. Sci. 58 (2003) 2215.
[111] S.O. Shekhtman, G.S. Yablonsky, J.T. Gleaves, R.R. Fushimi, Chem. Eng. Sci. 59 (2004) 5493.
[112] S.O. Shekhtman, G.S. Yablonsky, Ind. Eng. Chem. Res. 44 (2005) 6518–6522.
[113] B.S. Zou, M.P. Dudukovic, P.L. Mills, J. Catal. 148 (1994) 683.
[114] M. Rothaemel, M. Baerns, Ind. Eng. Chem. Res. 35 (1996) 1556.
[115] D.S. Lafyatis, G. Creten, O. Dewaele, G.F. Froment, Can. J. Chem. Eng. 75 (1997) 1100.
[116] G.S. Yablonskii, P. Phanawadee, J.T. Gleaves, I.N. Katz, Ind. Eng. Chem. Res. 36 (1997) 3149.
[117] P. Phanawadee, G.S. Yablonsky, P. Preechasanongkit, K. Somapa, Ind. Eng. Chem. Res. 38 (1999) 2877.
[118] D. Constales, G.S. Yablonsky, G.B. Marin, J.T. Gleaves, Chem. Eng. Sci. 56 (2001) 1913.
[119] D. Constales, G.S. Yablonsky, G.B. Marin, J.T. Gleaves, Chem. Eng. Sci. 56 (2001) 133.
[120] J.A. Delgado, T.A. Nijhuis, F. Kapteijn, J.A. Moulijn, Chem. Eng. Sci. 57 (2002) 1835.
[121] D.Z. Wang, Chem. Eng. Sci. 56 (2001) 3923.
[122] D.Z. Wang, J. Chin, Chem. Soc. 50 (2003) 551.
[123] D. Constales, G.S. Yablonsky, J.T. Gleaves, G.B. Marin, Chem. Eng. Sci. 59 (2004) 3725.
[124] D. Constales, S.O. Shekhtman, G.S. Yablonsky, G.B. Marin, J.T. Gleaves, Chem. Eng. Sci. 61 (2006) 6.
[125] G.F. Froment, K.B. Bischoff, Chemical Reactor Analysis and Design, 2nd edition, Wiley, New York, 1990.
[126] Y.S. Matros (Ed.), Unsteady-State Processes in Catalysis, VSP Press, Utrecht, The Netherlands, 1990.
[127] Y.S. Matros (Ed.), Proceedings of the 3rd International Conference on Unsteady-State Processes in Catalysis, VSP Press, Utrecht, The Netherlands, 1998.
[128] Y.S. Matros, G.A. Bunimovich, Ind. Eng. Chem. Res. 34 (1995) 1630.
[129] P.L. Mills, J.J. Lerou, Transient Response Methods for Assisted Design of Gas Phase Heterogeneous Catalysts: Experimental Techniques and Mathematical Modeling, Rev. in Chem. Eng., vol. 9, Freund Publishing House, Ltd, London, England, 1993, pp. 3–97.
[130] P.L. Silveston, Composition Modulation in Chemical Reactors, Cambridge University Press, Cambridge, England, 1997.
[131] P.L. Mills, W.E. Guise Jr., J. Chromatogr. Sci. 34 (1996) 431–459.
[132] P.L. Mills, J.F. Nicole, Ind. Eng. Chem. Res. 44 (2005) 6435–6452.
[133] P.L. Mills, J.F. Nicole, Ind. Eng. Chem. Res. 44 (2005) 6453–6465.
[134] P.L. Mills, J.F. Nicole, Ind. Eng. Chem. Res., in preparation.
[135] M.J. Lorences, G.S. Patience, F.V. Diez, J. Coca, Ind. Eng. Chem. Res. 42 (2003) 6730–6742.
[136] P. Perner, O. Salvetti (Eds.), Proceedings of the International Conference on Advances in Mass Data Analysis of Signals and Images in Medicine, Biotechnology, and Chemistry, MDA 2006/2007, Springer-Verlag, Leipzig, 2008 (Lecture Notes in Computer Science).
[137] R.J. Cotter, ACS Symposium Series, vol. 549, American Chemical Society, Washington, DC, 1994.
[138] W.G. Mallard, O.V. Toropov, Automatic Mass Spectral Deconvolution and Identification Software (AMDIS), Agilent Technologies, 2005.
[140] G. Centi, F. Cavani, F. Trifiro, Selective Oxidation by Heterogeneous Catalysis, Kluwer Academic and Plenum Publishers, New York, 2001, pp. 363–495.
[141] R.M. Contractor, U.S. Patent 5,021,588 assigned to E.I. DuPont de Nemours and Company, June 4, 1991.
[143] M.I. Temkin, Adv. Catal. 28 (1979) 173–291.
[144] M.I. Temkin, Int. Chem. Eng. 11 (1971) 709–717.
[145] M.I. Temkin, Kinet. Katal. 13 (1972) 555–565.
[146] K.G. Denbigh, J. Electrochem. Soc. 103 (1956) 137C.
[147] K.G. Denbigh, Am. J. Phys. 20 (1952) 385.
[148] G.S. Yablonsky, D. Constales, S.O. Shekhtman, J.T. Gleaves, Chem. Eng. Sci. 62 (2007) 6754–6767.
[149] R. Fushimi, X. Zheng, J.T. Gleaves, G.S. Yablonsky, A. Gaffney, M. Clark, S. Han, Top. Catal. 49 (2008) 167–177.
[150] P.L. Gai, K. Kourtakis, Science 267 (1995) 661–663.
[151] B.K. Hodnett, Catal. Rev. 27 (1985) 373–424.
[152] T.P. Moser, G.L. Schrader, J. Catal. 92 (1985) 216–231.
[153] J.M.C. Bueno, G.K. Bethke, M.C. Kung, H.H. Kung, Catal. Today 43 (1998) 101–110.
[154] S.T. Daniells, A.R. Overweg, M. Makkee, J.A. Moulijn, J. Catal. 230 (2005) 52–65.
[155] R.J. Berger, F. Kapteijn, J.A. Moulijn, G.B. Marin, J. De Wilde, M. Olea, D. Chen, A. Holmen, L. Lietti, E. Tronconi, Y. Schuurman, Appl. Catal. A: Gen. 342 (2008) 3–28.
[156] J.H.B.J. Huinink, J. Hoebink, G.B. Marin, Can. J. Chem. Eng. 74 (1996) 580–585.
[157] W.L.M. Weerts, M.H.J.M. de Croon, G.B. Marin, Surf. Sci. 367 (1996) 321–339.
[158] Anonymous, NIST/EPA/NIH Mass Spectral Library, 2nd edition, 2008, http://www.wiley.com/WileyCDA/WileyTitle/productCd-0470425180.html.
[159] K. Kourtakis, P.L. Mills, C.Z. Cao, US Patent 6,921,831 assigned to E.I. DuPont de Nemours and Company, July 26, 2005.
[160] O. Dewaele, V.L. Geers, G.F. Froment, G.B. Marin, Chem. Eng. Sci. 54 (1999) 4385.
[161] Y.J. Mergler, J. Hoebink, B.E. Nieuwenhuys, J. Catal. 167 (1997) 305.
[162] Y. Schuurman, Catal. Today 121 (2007) 187–196.
[163] S.O. Shekhtman, N. Maguiere, A. Goguet, R. Burch, C. Hardacre, Catal. Today 121 (3–4) (2007) 255–260.
[164] C.O. Bennett, AIChE J. 13 (1967) 890–895.
[165] H. Kobayashi, M. Kobayashi, Catal. Rev. -Sci. Eng. 10 (1974) 139–176.
[166] C.O. Bennett, Catalysis Under Transient Conditions, ACS Symposium Series 178, In: A.T. Bell, L.L. Hegedus (Eds.), American Chemical Society, Washington, DC, (1982) p. 1.
[167] C.O. Bennett, Adv. Catal. 44 (1999) 329–415.
[168] S.C. Van der Linde, T.A. Nijhuis, F.H.M. Dekker, F. Kapteijn, J.A. Moulijn, Appl. Catal. A: Gen. 151 (1997) 27.
[169] M. Olea, M. Kunitake, T. Shido, K. Asakura, Y. Iwasawa, Bull. Chem. Soc. Jpn. 74 (2001) 255.
[170] Y. Schuurman, J.T. Gleaves, Catal. Today 33 (1997) 25–37.
[171] Y. Schuurman, J.T. Gleaves, Ind. Eng. Chem. Res. 33 (1994) 2935–2941.